Modeling of Gravitational Waves

A thesis submitted towards partial fulfilment of
BS-MS Dual Degree Program

by

Ashok Choudhary

under the guidance of

Parameswaran Ajith

International Centre for Theoretical Sciences

Indian Institute of Science Education and Research
Pune

Certificate

This is to certify that this thesis entitled ”Modelling of Gravitational Waves from Binaries with Genric Spins” submitted towards the partial fulfilment of the BS-MS dual degree program at the Indian Institute of Science Education and Research Pune represents original research carried out by Ashok Choudhary at International Center for Theoretical Sciences, Tata Institute of Fundamental Research, Bengaluru, under the supervision of Prof. Parameswaran Ajith during the academic year 2013-2014.

Student	Supervisor
ASHOK	PARAMESWARAN
CHOUDHARY	AJITH

Acknowledgements

I'm very grateful to Prof. Parameswaran Ajith for agreeing to be my suppervior and guiding project work, and it has been a great experience. I forward my thanks to ICTS administration for their kind hospitality and nancial support during my stay at ICTS, Bangalore, and making my stay very comfortable and wonderful. I'm indebted to Prof. Suneeta vardarajan and Prof. Anil D. Gangal for their kind support and teaching which have been great learning experi- ence to me. I also forward my thanks to all other faculties at IISER Pune who have helped me grow as an individual and also as an student of Science.

I'm fortunate to have wonderful friends and batch, both outside and inside institue, who have tolerated me. Thanks to Dinesh, Kush, siddharth, vimlesh, Bhavesh, Shubham, Shivraj, Vikas, and many others with whom I have spent good, bad and ugly moments during these five years of stay at IISER Hostel and will certainly in future (as distance does not matter).

I forward my thanks to IISER administration and DST, Govt. of India, for provinding various facilities and support during these memorable and critical five years.

Abstract

Gravitational waves are the oscillations of gravitational field that propagate in space-time similar to light and radio waves which are propagating oscillations of electromagnetic fields. Gravitational waves are generated by accelerated masses. They can be detected using a pair of test masses. The detection is based on the principle that gravitational waves change the proper distance between the test masses as they pass through the space-time, just like a charged particle starts oscillating in response to an incoming electromagnetic wave.

The distortion caused by gravitational waves in the curvature of space-time are extremely small thus making it very difficult to detect them. However, with the current available technology it is possible to measure such small magnitudes of disturbances. The detectors employed for this purpose are the interferometric detectors. Examples of which include LIGO(Laser interferometric gravitational wave observatory) with detector facilities at Hanford, Washington, and Livingston, is Louisiana in the United States, and GEO600 near Sarstedt, Germany. Currently, these detectors have reached design sensitivities to probe such small disturbances.

For, detection of graviational waves in-spiralling black hole binaries are one of the most promising sources. These inspiralling Black hole binaries are the astrophysical objects which are expected to have significant spins. Non-alignment of the angular momentum with the individual Black hole spins gives rise to spin-orbit coupling. In order to compute the gravitational wave waveform in time domain we need to solve 11 coupled ODEs with appropriate boundary conditions. Later, for the purpose of detection and parameter estimations the Fourier domain waveform obtained by taking numerical FFT of time domain waveform is used.

In this work we obtain a Fourier domain waveform in a semi-analytical way using stationary phase approximation. Further, the number of differential equations in Fourier domain are brought down to 6 from 11 previously, as some of the equations reduce to algebraic equations. This approach followed by us is computationally less expensive than doing FFT of time domain waveform. We also compare our results with FFT of time domain waveform for different orientations of the binary system and observe that within our approxamation the method works well for low mass ratios of the binaries*eg.* $q = 1$ and $q = 4$. Our on going work focuses on improving this approximation and obtaining expression which works well for binaries with higher mass ratios.

Contents

Chapter 1

Introduction

Einstein's theory of General Relativity (GR) is a generalization of special relativity and Newton's law of gravitation. It provides a unified description of gravity as a geometrical property of space-time.
GR explains gravitation as a consequence of the curvature of space-time, while in turn curvature of space-time is a consequence of matter and radiation present. Thus, matter moves in response to the curvature of space-time consequently affecting the geometrical property and evolution of space-time. We can sum this up neatly in John Wheeler's words as:

Spacetime tells matter how to move
and matter tells spacetime how to curve

A metaphor generally used by people to describe gravity is shown in the figure 2.1. Let us first briefly consider Special Relativity and see how Einstein arrived at this remarkable theory of GR.

1.1 Geometry of spacetime

General relativity is generalization of special theory of relativity in which laws of physics are formulated in such a way that they are valid in all inertial frames. Here, inertial frames can described as all those frames in which Newton's first and second law holds, independent of their relative motion. Special relativity is formulated on fundamental postulate which says that, $s$peed of light is same for every inertial observer. As a consequence of this postulate, Einstein showed that the measurements in space and time can not be absolute, but they depend on the observers motion. Hence, Newtonian concept of a rigid framework of space and time against the physical phenomena were played out and were no longer tenable. Thus, the only quantity that

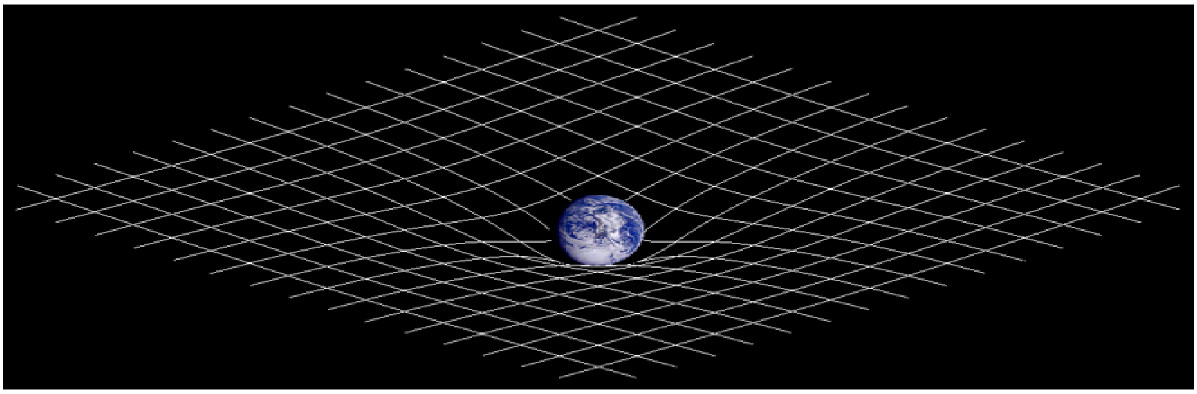

Figure 1.1: Familiar picture of spacetime as a stretched sheet of rubber, deformed by the presence of a massive body. A particle moving in the gravitational field of the central mass will follow a curved âĂŞ rather than a straight line âĂŞ trajectory as it moves across the surface of the sheet and approaches the central mass

remains independent of observers frame is the spacetime interval ds. This interval is the distance in space-time for the two neighbouring event taking place at spacetime coordinates $(t, x, y, z,)$ and $(t + dt, x + dx, y + dy, z + dz)$. It is defined as:-

$$ds^2 = -c^2dt^2 + dx^2 + dy^2 + dz^2 \tag{1.1}$$

Another inertial observer with different coordinate system (t', x', y', z') will find the same vale of interval.
The geometry described by 1.1 is called as the Minkowski spacetime. It differs from the flat Euclidian space geometry. Further, 1.1 can be written more generally as,

$$ds^2 = g_{\mu,\nu}dx^\mu dx^\nu \tag{1.2}$$

where, the repeated indices are summed over and the indices values run over 0,1,2,3, corresponding to t, x, y, z. In the above equation $g_{\mu\nu}$ are the components of the metric which tell us how the interval is measured in our spacetime. In general, these components can be complicated functions of spacetime coordinates depending upon the geometry of space. For Minkoswski spacetime, in Cartesian coordinates with setting c = 1, the metric takes a very simple form as shown below.

$$g_{\mu\nu} = diag(-1, 1, 1, 1) \tag{1.3}$$

Next important question we ask is how Newtonian gravity fits into a framework of Special Relativity? We can immediately see "it doesn't quite well!"

In Newtonian theory, gravitational force between two masses acts instantaneously and it depends on the spatial separation between the two massive object, which makes it non-relativistic. Different inertial observers in Newtonian framework will not agree upon the distances measured in different frames and hence will not measure same gravitational force between the objects. Next question that immediately comes to our mind is "How about non-inertial observer?". The geometry of Minkowski applies only to inertial observer with uniform relative motion, not to the accelerated motion. It was realized by Einstein that we need a fully covariant theory, describing the laws of physics (including gravity) in any co-ordinate system and for any relative motion. A crucial step towards achieving this goal came up with Einstein's thought of identifying the gravity with acceleration. This idea goes by the name of "Principal of Equivalence".

1.1.1 Equivalence principal

The Equivalence principal is presented in two forms which go by the names of weak equivalence principal and strong equivalence principal.

The weak equivalence principal

In Newtonian mechanics the mass(m_I) appearing in right hand side of Newton's second equation of motion is called inertial mass. It is the measure of resistance of a massive object to it's acceleration. The gravitational mass(m_G) of the body is mass that appears in the Newton's law of universal gravitation. These two masses are experimentally found to be equal to a very high precision. But, there is no priori reason, why these two masses have to be same.
The weak equivalence principal states that these two masses are identically equal.
Immediate consequence of it being that, a massive object freely falling in a uniform gravitational field will obey Newton's first and second law of motion. A freely falling frame object inhabits an inertial frame in which gravitational forces have disappeared. We can the refer to the frame inhabited by our freely-falling object as a local inertial frame(LIF). This frame is inertial over a region of spacetime where the gravitational field is uniform and for thus the nomenclature.

The strong equivalence principle

The Strong Equivalence Principle states that locally all the laws of physics have their usual special relativistic form except for gravity which simply disappears. Strong equivalence principal also claims that there is no way we can distinguish between the local inertial frame which is freely falling in a uniform gravitational field and an inertial frame which is in a region of the universe which is far away from matter.
Also, if we are inside a spaceship in a region free of gravity, it is possible simulate gravity by giving the rocket an acceleration. The acceleration given is indistinguishable from a uniform gravitational field but it is equal and opposite to gravitational acceleration.

1.2 From Special to General Relativity

Provided our gravitational field is uniform, equivalence principal tells us that we can define a local inertial frame: a coordinate system within which gravity has simply disappeared. In this frame the laws of physics agree with Special Relativity and the metric can be reduced to simple Minkowski form. This is the first step towards a fully covariant theory of gravity.
Gravitational fields are in general not uniform(two inertial frames at two different location are very different!). So, we can only transform away their effect locally.
In order to build an effective theory of gravity, we need to stitch together these local inertial frames across extended region of spacetime, containing non-uniform fields. This stitching together turns the locally flat geometry of Minkowski spacetime into the curved geometry that characterises the gravitational field of extended regions.

1.2.1 Einstein's equations

Einstein's field equations are a set of 10 equations that describe the fundamental interaction of gravitation as a result of spacetime being curved by matter and energy.
In an analogy to electromagnetic theory where electromagnetic fields are determined using charges and current via maxwell's equations, Einstein's field equations are used to determine the spacetime geometry resulting from the presence of matter-energy and linear momentum. These equations determine the metric tensor of spacetime for a given arrangement of stress-energy in the spacetime.

The Einstein's field equations can be written as:

$$R_{\mu\nu} - \frac{1}{2}g_{\mu\nu}R + g_{\mu\nu}\Lambda = \frac{8\pi G}{c^4}T_{\mu\nu} \tag{1.4}$$

where, $R_{\mu\nu}$ is the Ricci curvature tensor, R the scaler curvature, $g_{\mu\nu}$ the metric tensor, Λ, G is the Newtonian gravitational constant, c the speed of light in vacuum, and $T_{\mu\nu}$ the stress-energy tensor. The left hand side of 1.4 is a function of metric $g_{\mu\nu}$ and its derivatives. The right had side of the same is determined by a source term.

1.2.2 Wave Equation for Gravitational Radiation

Let us look for the solutions to the equation 1.4 with metric perturbations of a nearly flat spacetime in free space with cosmological constant(Λ) set to zero.

'Nearly' flat spacetimes

In the absence of gravitational field the spacetime is flat, in which case the metric describing the geometry is given by Minkowski metric. A nearly flat space time is described by a metric that takes the form given below, in some co-ordinate systems.

$$g_{\mu\nu} = \eta_{\mu\nu} + h_{\mu\nu} \tag{1.5}$$

where,

$$\eta_{\mu\nu} = diag(-1, 1, 1, 1) \tag{1.6}$$

is the Minkowski metric of Special Relativity, and $h_{\mu\nu} \ll 1$ for all μ and ν

A coordinate system satisfying 1.5 and 1.6 is referred to as nearly Lorentz coordinate system. It is always possible to find a coordinate system in which a nearly flat spacetime takes the form given by 1.5, but this does not mean the metric will be of this form in any coordinate system.
Also, the coordinate system in which one may express the metric component of a nearly flat spacetime in the form of 1.5 and 1.6 is certainly not unique. If we have found one coordinate system in which metric takes such form, then we can find an infinite family of others by carrying out particular coordinate transformations. The coordinate transformations which preserve the properties of 1.5 and 1.6 are known as Background Lorentz transformations and Gauge transformations.

Background Lorentz transformations

Let us suppose we are in Minkowski spacetime of Special relativity and we define the inertial frame, X whose coordinates are given by (t, x, y, z). Now, suppose we transform to another coordinate system, X', corresponding to a Lorentz boost of speed v in the direction of the positive x-axis. New coordinates in X' under the Lorentz transformation are given by

$$(t', x', y', z')^T = \begin{pmatrix} \gamma & -v\gamma & 0 & 0 \\ -v\gamma & \gamma & 0 & 0 \\ 0 & 0 & 1 & 0 \\ 0 & 0 & 0 & 1 \end{pmatrix} (t, x, y, z)^T \tag{1.7}$$

where, $\gamma = (1 - v^2)^{-1/2}$. We have set $c = 1$ for simplicity.Above equation can be written in a more compact form as

$$x'^\alpha = \Lambda^{\alpha'}_\beta x^\beta \equiv \frac{\partial x'^\alpha}{\partial x^\beta} x^\beta \tag{1.8}$$

Now let us assume we are in a nearly flat spacetime, where we have identified nearly Lorentz coordinates (t, x, y, z) satisfying 1.5 and 1.6 .In this new coordinate system the metric component takes the form.

$$g'_{\alpha\beta} = \Lambda^\mu_{\alpha'} \Lambda^\nu_{\beta'} g_{\alpha\beta} = \frac{\partial x^\mu}{\partial x'^\alpha} \frac{\partial x^\nu}{\partial x'^\beta} g_{\mu\nu} \tag{1.9}$$

Substituting from 1.5 we can write this as

$$g'_{\alpha,\beta} = \eta'_{\alpha\beta} + \frac{\partial x^\mu}{\partial x'^\alpha} \frac{\partial x^\nu}{\partial x'^\beta} h_{\mu\nu} = \eta_{\alpha\beta} + h'_{\alpha\beta} \tag{1.10}$$

The last follows from the fact that the component on the Minkowski metric are the same in any Lorentz frame.
If we consider only transformation given by 1.7, the component of $h_{\mu\nu}$ transform as if they are the component of a (0,2) tensor defined on the background flat spacetime. Now provided that $v \ll 1$, then if $|h_{\alpha\beta}| \ll 1$ for all α and β , then $|h'_{\alpha\beta}| \ll 1$ also.

Space time which looks nearly flat to one observer will also look flat to an observer moving with constant relative motion with respect to fist observer.

Gauge transformations

Now, suppose we make a very small change in our coordinate system by applying a coordinate transformation of the form

$$x'^\alpha = x^\alpha + \zeta^\alpha(x^\beta) \tag{1.11}$$

Here the components of ζ^α are function of coordinates $\{x^\beta\}$. It follows immediately that

$$\frac{\partial x'^\alpha}{\partial x^\beta} = \delta^\alpha_\beta + \zeta^\alpha_{,\beta} \tag{1.12}$$

using 1.11 we can also write

$$x^\alpha = x'^\alpha - \zeta^\alpha(x^\beta) \tag{1.13}$$

Now demanding ζ^α and it's derivative to be small, which means

$$|\zeta^\alpha_{,\beta}| \ll 1 \ \text{ for all } \ \alpha, \beta \tag{1.14}$$

we can see using chain rule that

$$\frac{\partial x^\alpha}{\partial x'^\gamma} = \delta^\alpha_\gamma - \frac{\partial x^\beta}{\partial x'^\gamma}\frac{\partial \zeta^\alpha}{\partial x^\beta} \ \simeq \ \delta^\alpha_\gamma - \zeta^\alpha_{,\gamma} \tag{1.15}$$

where we have used the fact that Kronecker delta are same in any coordinate frame and terms higher then first order are neglected.

Let us now take our unprimed coordinate to be nearly Lorentz and make a coordinate transformation to primed coordinate system. Our metric being a tensor transforms the following way.

$$g'_{\alpha\beta} = \frac{\partial x^\mu}{\partial x'^\alpha}\frac{\partial x^\nu}{\partial x'^\beta} g_{\mu\nu} \tag{1.16}$$

Neglecting terms higher in order then first order after substituting from 1.5 and 1.15 above equation becomes.

$$g'_{\alpha\beta} = (\delta^\mu_\alpha \delta^\nu_\beta - \zeta^\mu_{,\alpha}\delta^\nu_\beta - \zeta^\nu_{,\beta}\delta^\mu_\alpha)\eta_{\mu\nu} + \delta^\mu_\alpha \delta^\nu_\beta h_{\mu\nu} \tag{1.17}$$

On further simplification

$$g'_{\alpha\beta} = \eta_{\alpha\beta} + h_{\alpha\beta} - \zeta_{\alpha,\beta} - \zeta_{\beta,\alpha} \tag{1.18}$$

In the above equation we have used

$$\zeta_\alpha = \eta_{\alpha\nu}\zeta^\nu \tag{1.19}$$

We have used the Minkowski metric, rather than the full metric $g_{\mu\nu}$ to lower the index, which is allowed because we are keeping only first order terms. Both the metric perturbation $h_{\mu\nu}$ and the component ζ^ν are very small.

Equation 1.18 has the same form as 1.5 provided that we take

$$h'_{\alpha\beta} = h_{\alpha\beta} - \zeta_{\alpha,\beta} - \zeta_{\beta,\alpha} \tag{1.20}$$

And so we observe that our new coordinate system is also nearly Lorentz. Once we have identified a coordinate system which is nearly Lorentz, we can make infinitesimal coordinate transformation by adding a small vector ζ^α which will take us to another nearly Lorentz spacetime. We will use this freedom to simplify our Einstein's equations.

Einstein's equations for a weak gravitational field

Einstein's equation is simplified considerably if work in nearly flat spacetime. This choice eventually lead us to spot that the derivations from the metric of Minkowski spacetime - the component $h_{\alpha\beta}$ in 1.5 - obey a wave equation. If we compute left hand side of Einstein's equation and set cosmological constant(Λ) to zero, we reach at the following result

$$G_{\mu\nu} = \frac{1}{2}[h_{\mu\alpha,\nu}{}^{,\alpha} + h_{\nu\alpha,\mu}{}^{,\alpha} - h_{\mu\nu,\alpha}{}^{,\alpha} - h_{,\mu\nu} - \eta(h_{\alpha\beta}{}^{,\alpha\beta} - h_{,\beta}{}^{;\beta})] \tag{1.21}$$

The above messy looking expression can be simplified by introducing a modified perturbation defined by

$$\bar{h}_{\mu\nu} \equiv h_{\mu\nu} - \frac{1}{2}\eta_{\mu\nu}h \tag{1.22}$$

where $h \equiv h^\alpha_\alpha = \eta^{\alpha\beta}h_{\alpha\beta}$ and after making the above substitution, equation 1.21 becomes

$$G_{\mu\nu} = -\frac{1}{2}\left[\bar{h}_{\mu\nu,\alpha}{}^{,\alpha} + \eta_{\mu\nu}\bar{h}_{\alpha\beta}{}^{,\alpha\beta} - \bar{h}_{\mu\alpha,\nu}{}^{\alpha} - \bar{h}_{\nu\alpha,\mu}{}^{\alpha}\right] \tag{1.23}$$

We can now write down the Einstein's equations in their linearised, fully covariant form for weak gravitational fields, in terms of the(rescaled) metric perturbation $\bar{h}_{\mu\nu}$. We have

$$G_{\mu\nu} = 8\pi T_{\mu\nu} \tag{1.24}$$

it follows from above that

$$-\bar{h}_{\mu\nu,\alpha}{}^{,\alpha} - \eta_{\mu\nu}\bar{h}_{\alpha\beta}{}^{,\alpha\beta} + \bar{h}_{\mu\alpha,\nu}{}^{\alpha} + \bar{h}_{\nu\alpha,\mu}{}^{\alpha} = 16\pi T_{\mu\nu} \tag{1.25}$$

Further simplification to the above equation can be made by choosing an appropriate gauge conditions. With some work it can shown that, it is possible to a carry out a gauge transformation in a nearly Lorentz coordinate system and the new coordinate system is still nearly Lorentz, with (to the first order) identical curvature. We can choose the gauge condition given by equation below

$$\bar{h}^{\mu\alpha}{}_{,\alpha} = 0 \tag{1.26}$$

This gauge transformation is called Lorentz gauge.In this gauge, the Einstein's equation reduces to the somewhat simpler form.

$$-\bar{h}_{\mu\nu,\alpha}{}^{;\alpha} = 16\pi T_{\mu\nu} \tag{1.27}$$

Solution to Einstein's equations in free space

In the free space the energy momentum tensor is identically zero. The free space solutions of equation (1.27) are solutions to the equation

$$\bar{h}_{\mu\nu,\alpha}{}^{;\alpha} = 0 \tag{1.28}$$

With some further simplification and putting back c for the speed of light, we reach at the equation given below

$$\Big(-\frac{\partial^2}{\partial t^2} + c^2 \bigtriangledown^2\Big)\bar{h}_{\mu\nu} = 0 \tag{1.29}$$

The above equation has a mathematical form of wave equation. This equation tell us that the metric perturbation of spacetime propagate with the speed of light.

With further gauge conditions it can be shown that a coordinate system can be chosen in which the 16 component of a linear metric perturbation reduces to only 2 independent components. We call this gauge Transverse-Traceless Gauge.

The metric perturbation in TT gauge look like

$$\bar{h}^{(TT)}_{\mu\nu} = \begin{pmatrix} 0 & 0 & 0 & 0 \\ 0 & \bar{h}^{(TT)}_{xx} & \bar{h}^{(TT)}_{xy} & 0 \\ 0 & \bar{h}^{(TT)}_{xy} & -\bar{h}^{(TT)}_{xx} & 0 \\ 0 & 0 & 0 & 0 \end{pmatrix} \tag{1.30}$$

-

Chapter 2

Theory

In this chapter we discuss about detection of gravitational waves from binary black hole system.

2.1 Gravitational waves from binary black hole system

Among the most promising source for gravitational wave detection by Laser interferometric detector like LIGO, Virgo, GEO 600 are the coalescing compact binaries which consist of stellar mass/intermediate-mass black holes and neutron stars. These compact binaries can be produced in various astrophysical scenarios. These scenarios can be grouped into two main classes :1 One of the possibility where formation of such a binary system can take place is through supernova explosion of a massive binary star system. Here two start constituting binary under go successive supernova explosions with out disrupting the orbit of the system. 2 Another interesting scenario where formation of such a binary can take place is two compact object forming a bound orbit due to dynamical interaction in dense interstellar medium.After the binary system is formed it evolves by radiating gravitational waves and the individual masses in-spiral and finally merge with each other.

These binary systems are expected to have sufficient spin which is indicated by the spin measurement of stellar-mass black hole($||S||/m^2$ $0.2-0.98$). In general if the binary system is formed in isolated evolution, it spins are expected to be nearly aligned with total angular momentum. The distribution of spin tilt angles(the angle between the spins and total angular momentum) depends upon the distribution of supernova kicks. The binaries which are formed due to the dynamical interaction have no particular pre-distribution of tilt angles. If the spins are not aligned with the orbital angular momen-

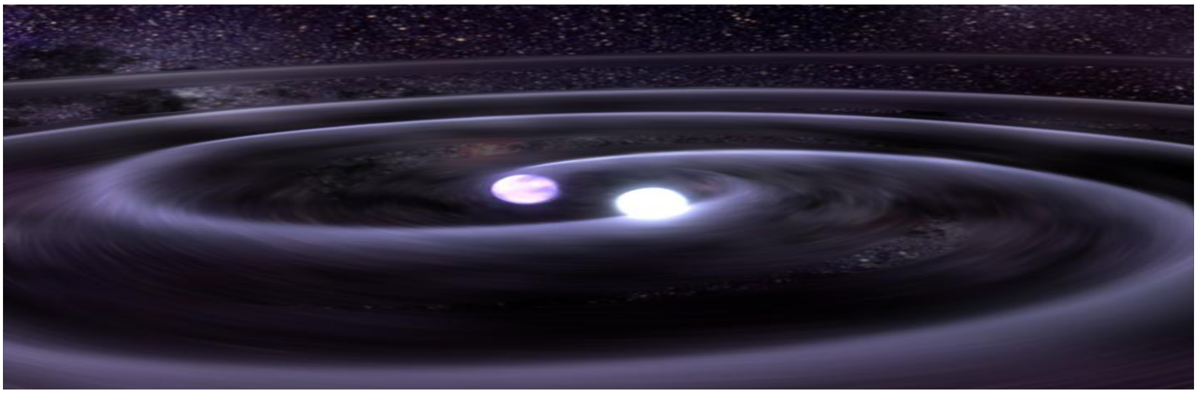

Figure 2.1:

tum, the general relativistic spin-spin and spin-orbit coupling causes spins to precess around the direction of the total angular momentum. This spin-orbit and spin-spin coupling adds up an addition complexity in the gravitational wave signals.

The gravitational wave produced by these compact binary sources are buried in Laser Interferometric detector's noisy data. The signal are extracted using the best known technique for data analysis called match filtering. This technique involves cross-correlating data with expected gravitational waveform. The expected gravitational waveforms are constructed by solving the Einstein's equation numerically or using approximate analytical method. In the initial evolution phase of binary when the individual mass are not moving with relativistic speed($v/c << 1$),the waveform obtained by pos-Newtonian approximation to general relativity gives good enough waveforms for data analysis purpose. In the ultra-relativistic regime post-Newtonian approximation breaks down,at this stage more accurate waveforms are needed, which are obtained by solving the solving Einstein's equation exactly using numerical simulations.

A hybrid waveform can be constructed by combining the early in-spiral part post-Newtonian waveform and the later merger, ring down waveform obtained using numerical relativity simulations. For the binaries with low mass ratio($m_1 + m_2 \lessapprox M_\odot$), the signal to noise is almost entirely contributed by in-spiral portion of signal for which post-Newtonian theory works well. The expected form of signal is a function of source parameter which are not known priori. These parameters are buried into the noisy data of signal which can be estimated by cross correlating the data with a "bank" of theoretical templates corresponding to different(astrophysically plausible) values of physical parameters. A geometrical formalism has been developed for "laying down" the templates in the parameter space of compact binaries. Various templates in the template bank are chosen in such a way that the parameters in any two neighbouring template is less than an acceptable value, while at the same time keeping the total number of template employed in the search computationally tractable.

The templates for spinning binaries are characterized by a set of total 10 parameters which includes masses of two individual black holes, total six components of spin vectors, and two for inclination angle and polarization angle. These many parameters makes it very complicated to place these templates in the bank and it also increase the computational cost in parameter estimations by a considerable amount. Many of the configurations of spins are known to be degenerate which makes it unnecessary to put templates corresponding to all these configuration in the bank.

In order to reduce the computational cost it is important to construct an effective template family parametrized by a small number of parameters that has high enough overlap with the expected signals. Buonanno, Chen and Vallisneri(BCV) proposed a phenomenological template family that has a very good overlap with the target signals, by introducing modulation effect in both frequency domain amplitude and phase. Several of these phenomenological template family could be searched over which reduced the computational cost significantly. These phenomenological template family were used to look for gravitational waves from spinning binaries using the data from LIGO's third science run. The sensitivity of this search towards spinning binary was found to be not better then a search employing non-spinning templates. The reason for this was that the increased number of degree of freedom associated(due to analytical maximization of several phenomenological parameters) with the detection statistic also increased the false alarm rate.Later on it was demonstrated by Van Den Broeck that, although BCP templates have high overlap with the target signal, the increased degree of freedom associated with the detection statistics and the lack of good method for vetoing non-Gaussian detector glitches that mimic the expected signal resulted in producing a much higher false alarm rate in the presence of non-Gaussian noise, and hence negated the advantages.

A better physical template is suggested by BVC, which presumably will not suffer from the limitations described above. This template family assumes that only one compact object has significant spin. This template family is parametrized by four parameters that need to be searched over, which include two masses, magnitude of single spin and spin tilt angle. This template family has be extensively studied by Pan and Buananno, where they have demonstrated that this template family is effectual in detecting single spin as well as double-spin binaries using initial detectors. It has also been demonstrated that there is a possibility of reducing the number of spin parameters to one in certain region parameter space. This template has been implemented in the LIGO-Virgo search pipe lines.

In this work, we present a semi-analytic frequency-domain post-Newtonian waveform family for generic spinning binaries.

2.1.1 POST-NEWTONIAN WAVEFORMS IN THE ADIABATIC APPROXIMATION

In this discussion, only the binaries with quasi circular orbits are considered. It is expected that the inspiralling compact binaries loose their eccentricity before GW signals reach near the sensitivity of ground based detectors. In the early inspiral period of compact binary due the emission of GW, the change in the orbital frequency is much smaller than the orbital frequency itself. During this adiabatic inspiral period, the loss of the specific orbital binding energy $E(v)$ (binding energy per unit mass) is related to energy flux of gravitational waves $\mathcal{F}(v)$ in the following way: $mdE(v)/dt = \mathcal{F}(v)$. The energy balance argument provides the following coupled ordinary differential equations which can be used determines the evolution of orbital phase $\varphi(t)$.

$$\frac{d\varphi}{dt} = \frac{v^3}{m} \tag{2.1}$$

$$\frac{dv}{dt} = -\frac{\mathcal{F}(v)}{mE'(v)} \tag{2.2}$$

In the above equations, v is the velocity parameter which is related to the orbital frequency ω by $v = (\omega m)^{1/3}$ where $m = m_1 + m_2$ is the total mass of the binary, and $E'(v) = dE/dv$.The energy and flux function are then computed as PN expansion of small parameter v. At present we have energy and flux function upto $3(v^6)$, $3.5(v^7)$ PN respectively: but the spin effects are computed only upto 2 PN and 2.5 PN only in energy and flux expressions respectively.

$$
\begin{aligned}
\frac{E'(v)}{\mathcal{F}(v)} =& \frac{-5}{32v^9\eta}\Bigg\{1+v^2\left[\frac{11\eta}{4}+\frac{743}{336}\right]+v^3\left[\frac{113}{12}\left(\left(1-\frac{76\eta}{113}\right)\boldsymbol{\chi_s}.\hat{\boldsymbol{L}}_N+\delta\boldsymbol{\chi_a}.\hat{\boldsymbol{L}}_N\right)-4\pi\right]\\
&+v^4\left[(\boldsymbol{\chi_a}.\hat{\boldsymbol{L}}_N)^2\left(30\eta-\frac{719}{96}\right)-\frac{719\boldsymbol{\chi_a}.\hat{\boldsymbol{L}}_N\boldsymbol{\chi_s}.\hat{\boldsymbol{L}}_N\delta}{48}+\boldsymbol{\chi_a}^2\left(\frac{233}{96}-10\eta\right)\right.\\
&+6\frac{233\boldsymbol{\chi_a}\cdot\boldsymbol{\chi_s}\delta}{48}+(\boldsymbol{\chi_s}.\hat{\boldsymbol{L}}_N)^2\left(-\frac{\eta}{24}-\frac{719}{96}\right)+\boldsymbol{\chi_s}^2\left(\frac{7\eta}{24}+\frac{233}{96}\right)+\frac{617\eta^2}{144}\\
&\left.+\frac{5429\eta}{1008}+\frac{3058673}{1016064}\right]+v^5\left[\boldsymbol{\chi_a}.\hat{\boldsymbol{L}}_N\delta\left(\frac{7\eta}{2}+\frac{146597}{2016}\right)+\boldsymbol{\chi_s}.\hat{\boldsymbol{L}}_N\left(-\frac{17\eta^2}{2}\right.\right.\\
&\left.\left.-\frac{1213\eta}{18}+\frac{146597}{2016}\right)+\frac{13\pi\eta}{8}-\frac{7729\pi}{672}\right]+v^6\left[\frac{1712\gamma_E}{105}+\frac{25565\eta^3}{5184}-\frac{15211\eta^2}{6912}\right.\\
&\left.-\frac{451\pi^2\eta}{48}+\frac{3147553127\eta}{12192768}+\frac{32\pi^2}{3}-\frac{10817850546611}{93884313600}+\frac{1712\ln(4v)}{105}\right]\\
&+v^7\left[\frac{1480\pi\eta^2}{3024}-\frac{75703\pi\eta}{6084}-\frac{154193335\pi}{1016064}\right]\Bigg\}.
\end{aligned}
\tag{2.3}
$$

In the above equation, $\eta \equiv m_1m_2/m^2$ is the symmetric mass ratio, $\delta \equiv (m_1-m_2)/m$ the asymmetric mass ratio, γ_E the Euler's constant, and $\hat{\boldsymbol{L}}_N$ the unit vector along the Newtonian orbital angular momentum $\boldsymbol{L}_N \equiv m^2\eta/v\hat{\boldsymbol{L}}_N$. The spin variable $\boldsymbol{\chi_s}$ and $\boldsymbol{\chi_a}$ are related to the(dimensionless) spin vector of the binary as:

$$
\boldsymbol{\chi}_s = (\boldsymbol{\chi}_1+\boldsymbol{\chi}_2)\,, \qquad \boldsymbol{\chi}_a = (\boldsymbol{\chi}_1-\boldsymbol{\chi}_2) \tag{2.4}
$$

where $\boldsymbol{\chi}_i \equiv \boldsymbol{S}_i/{m_i}^2$, $\boldsymbol{S_i}$ is the spin angular momentum of ith compact binary. Using the equation 2.2, 2.2, 2.3 we can obtain the explicit expression of orbital phase as a function of v, which is as follow:

$$
\begin{aligned}
\varphi(v) =&\varphi_0 - \frac{1}{32v^5\eta}\Bigg\{1 + v^2\left[\frac{55\eta}{12} + \frac{3715}{1008}\right] + v^3\left[\frac{565}{24}\left(\left(1-\frac{76\eta}{113}\right)\boldsymbol{\chi}_s.\hat{\boldsymbol{L}}_N + \delta\boldsymbol{\chi}_a.\hat{\boldsymbol{L}}_N\right) - 10\pi\right]\\
&v^4\Bigg[(\boldsymbol{\chi}_a.\hat{\boldsymbol{L}}_N)^2\left(150\eta - \frac{3595}{96}\right) - \frac{3595\boldsymbol{\chi}_a.\hat{\boldsymbol{L}}_N\hat{\boldsymbol{\chi}}_s.\boldsymbol{\chi}_N\delta}{48} +\\
&\boldsymbol{\chi}_a^2\left(\frac{1165}{96} - 50\eta\right) + \frac{1165\boldsymbol{\chi}_s.\boldsymbol{\chi}_a\delta}{48} + (\boldsymbol{\chi}_s.\hat{\boldsymbol{L}}_N)^2\left(-\frac{5\eta}{24} - \frac{3595}{96}\right) +\\
&\boldsymbol{\chi}_s^2\left(\frac{35\eta}{24} + \frac{1165}{96}\right) + \frac{3085\eta^2}{144} + \frac{27145\eta}{1008} + \frac{15293365}{1016064}\Bigg]\\
&+ v^5\Bigg[\Bigg(\boldsymbol{\chi}_a.\hat{\boldsymbol{L}}_N\left(-\frac{35\delta\eta}{2} - \frac{7329855\delta}{2016}\right) + \boldsymbol{\chi}_s.\hat{\boldsymbol{L}}_N\Bigg(\frac{85\eta^2}{2} + \frac{6065\eta}{18} -\\
&\frac{732985}{2016}\Bigg) - \frac{65\pi\eta}{8} + \frac{38645\pi}{672}\Bigg)\ln(v)\Bigg] + v^6\Bigg[-\frac{127825\eta^3}{5184} + \frac{76055\eta^2}{6912} + \frac{2255\pi^2\eta}{48} -\\
&\frac{15737765635\eta}{12192768} - \frac{1712\gamma_E}{21} - \frac{160\pi^2}{3} + \frac{12348611926451}{18776862720} - \frac{1712\ln(4v)}{21}\Bigg] +\\
&v^7\Bigg[-\frac{74045\pi\eta^2}{6048} + \frac{378515\pi\eta}{12096} +\\
&\frac{77096675\pi}{2032128}\Bigg]\Bigg\},
\end{aligned}
\tag{2.5}
$$

where φ_0 is some initial reference phase.

We can reduce the phasing formula into one differential equation describing the evolution of orbital frequency and one explicit expression of orbital phase as function of v.

$$
\frac{dv}{dt} = \left[\frac{-mE'(v)}{\mathcal{F}(v)}\right]^{-1}, \quad \varphi(v) = \varphi_0 - \frac{1}{32v^5\eta}\Bigg\{1 + ...\Bigg\} \tag{2.6}
$$

This particular way of solving phasing formula is called “TaylorT5”. There are many different ways in which the time dependent phasing formula can be obtained, and we call them different Taylor (i.e. TaylorT1, TaylorT2, TaylorT3 etc.) approximates. This Taylor approximate(TaylorT5) has an advantage over other Taylor approximation that here only one differential

equation need to be solved numerically and: the phasing formula is computed as an explicit expansion in v. Additionally, since the spin dependent terms in the PN expansion of the energy and flux function are available only up to a rather low 2.5 PN order,the different approximations gives different results. We are interested in isolating this issue from issue of the effect of spin-precession in the target signals. The target waveform are constructed in such a way that they are as close to the non-precessing frequency- domain template family as possible in the limit of non-precessing spins. In order to achieve this the same expansion of $\frac{E'(v)}{\mathcal{F}(v)}$. is used to construct both the time domain and Fourier domain waveform.
If the spin vectors of the binary not aligned along the orbital angular momentum, the spin-spin and spin-orbit coupling cause the spin and orbital angular momentum to precess around the nearly constant direction of total angular momentum J. This lead to constantly changing the angle between the spins and angular momentum. The equations governing the dynamics of spin and orbital angular momentum are as follows:

$$\frac{m^2\eta}{v}\left[1+\left(\frac{3}{2}+\frac{\eta}{6}\right)v^2\right]\frac{d\hat{\boldsymbol{L}}_N}{dt} = -\frac{d}{dt}(\boldsymbol{S}_1+\boldsymbol{S}_2) \tag{2.7}$$

and

$$\frac{d\boldsymbol{S}_i}{dt} = \boldsymbol{\Omega}_i \times \boldsymbol{S}_i,\ i=1,2 \tag{2.8}$$

where

$$\begin{aligned}\boldsymbol{\Omega}_1 =& \frac{v^5}{m}\Bigg\{\left(\frac{3}{4}+\frac{\eta}{2}-\frac{3\delta}{4}\right)\hat{\boldsymbol{L}}_N+\frac{v}{2m^2}\big[-3(\boldsymbol{S}_2+q\boldsymbol{S}_1).\hat{\boldsymbol{L}}_N\hat{\boldsymbol{L}}_N+\boldsymbol{S}_2\big]\\ & v^2\left(\frac{9}{16}+\frac{5\eta}{4}-\frac{\eta^2}{24}-\frac{9\delta}{16}+\frac{5\delta\eta}{8}\right)\hat{\boldsymbol{L}}_N\Bigg\},\end{aligned} \tag{2.9}$$

$$\begin{aligned}\boldsymbol{\Omega}_2 =& \frac{v^5}{m}\Bigg\{\left(\frac{3}{4}+\frac{\eta}{2}+\frac{3\delta}{4}\right)\hat{\boldsymbol{L}}_N+\frac{v}{2m^2}\big[-3(\boldsymbol{S}_1+q^{-1}\boldsymbol{S}_2).\hat{\boldsymbol{L}}_N\hat{\boldsymbol{L}}_N+\boldsymbol{S}_1\big]\\ & v^2\left(\frac{9}{16}+\frac{5\eta}{4}-\frac{\eta^2}{24}+\frac{9\delta}{16}-\frac{5\delta\eta}{8}\right)\hat{\boldsymbol{L}}_N\Bigg\}\end{aligned} \tag{2.10}$$

Here in the above equations, $q \equiv m_2/m_1$ and $\|\boldsymbol{\Omega}_i\|$ is the instantaneous precession frequency of the individual spins.

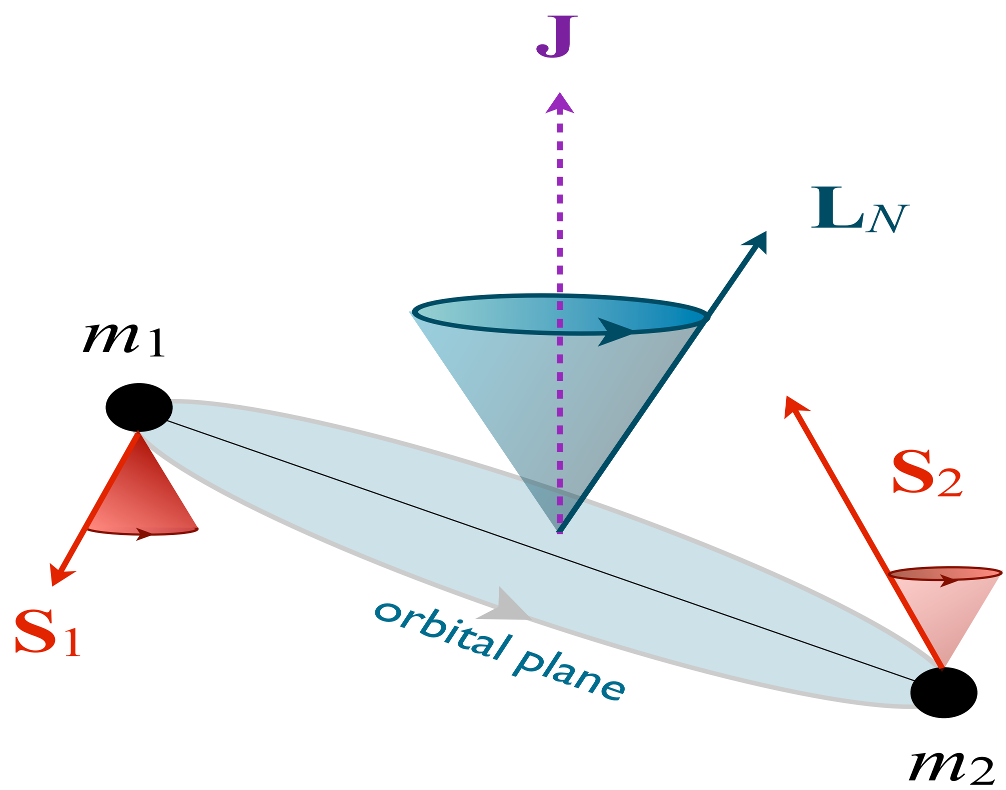

Figure 2.2: Above figure shows precession of orbital plain due to spin-orbit coupling

The spins and orbital angular momentum can be evolved by solving the above set of coupled ODEs numerically. The evolution of these quantities is solved in the coordinate proposed by Finn and Chernoff. The figure on page 21 describes the Finn Chernoff coordinate system. In this co-ordinate system the direction of z axis is determined by the direction of initial total angular momentum $\boldsymbol{J} \approx \boldsymbol{L}_N + \boldsymbol{S}_1 + \boldsymbol{S}_2$ and x axis is chosen such that the detector lies in x-y plain .

In case of non-precessing binaries the GW phase is twice the orbital phase. But the presence of precession in orbital phase introduces additional modulation in the orbital phase. If we define orbital phase as $\Phi(t)$ then the phase evolution of GW is 2Φ(t). Where Φ(t) is given by

$$\frac{d\Phi}{dt} = \omega - \frac{d\alpha}{dt} \cos i, \tag{2.11}$$

where α and i are the angles that describes the evolution of orbital angular

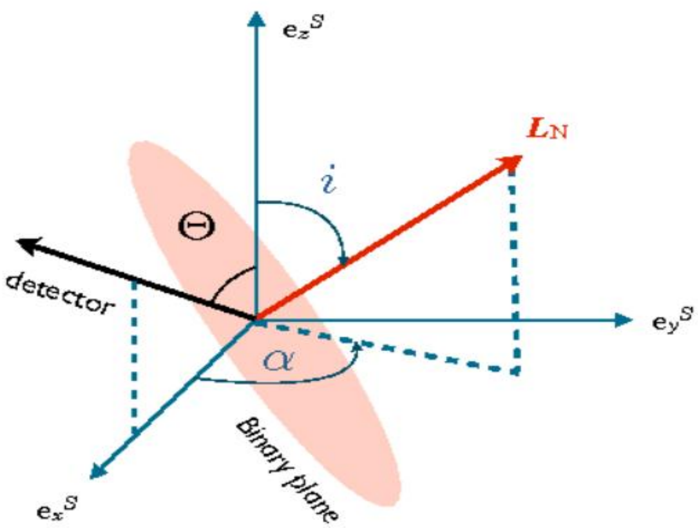

Figure 2.3: Source frame in the Finn-Chernoff convention. The z-axis points to the direction of the initial total angular momentum vector J, the detector lies in the x - z plane, and the angles α and i describe the evolution of the orbital angular momentum vector LN in the source frame

momentum.

$$\alpha = \arctan(\hat{L}_{N_y}/\hat{L}_{N_x}), \quad i = \arccos(\hat{L}_{N_z}) \tag{2.12}$$

The gravitational wave observed in the detector frame can be written as:

$$h(t) = C_Q(t)\cos 2[\Phi(t) + \Phi_0] + S_Q(t)\sin 2[\Phi(t) + \Phi_0] \tag{2.13}$$

where

$$\begin{aligned} C_Q(t) &= -\frac{4\eta m}{D} v^2 [C_+(t)F_+ + C_\times(t)F_\times], \\ S_Q(t) &= -\frac{4\eta m}{D} v^2 [S_+(t)F_+ + S_\times(t)F_\times], \end{aligned} \tag{2.14}$$

here, Φ_0 is the constant that depends upon the initial configuration of Binary. D in the above equation is the luminosity distance of the binary and F_+, $F_\times$ are the antenna pattern functions.

$$\begin{aligned} F_+ &= \frac{1}{2}(1+\cos^2\theta)\cos 2\phi \cos 2\psi - \cos\theta \sin 2\phi \sin 2\psi \\ F_\times &= \frac{1}{2}(1+\cos^2\theta)\cos 2\phi \cos 2\psi + \cos\theta \sin 2\phi \sin 2\psi \end{aligned} \tag{2.15}$$

where θ and ϕ are the polar and the azimuth angles that specify the position of the binary in the detectors frame, ans ψ is the polarization angle.

$$
\begin{aligned}
C_+(t) =& \frac{1}{2}\cos^2\Theta(\sin^2\alpha - \cos^2 i\cos^2\alpha) + \frac{1}{2}(\cos^2 i\sin^2\alpha - \cos^2\alpha) \\
& - \frac{1}{2}\sin^2\Theta\sin^2 i - \frac{1}{4}\sin 2\Theta\sin 2i\cos\alpha \\
S_+(t) =& \frac{1}{2}(1+\cos^2)\cos i\sin 2\alpha + \frac{1}{2}\sin 2\Theta \\
C_\times(t) =& -\frac{1}{2}\cos\Theta(1+\cos^1 i)\sin 2\alpha - \frac{1}{2}\sin\Theta\sin 2i\sin\alpha, \\
S_\times(t) =& -\cos\Theta\cos i\cos 2\alpha - \sin\Theta\sin i\cos\alpha
\end{aligned}
\tag{2.16}
$$

where Θ is the angle between the line of sight from the detector to the source and the z-axis of the coordinate system.
The time dependent GW signal observed in the detector frame is given by:

$$h(t) = A(t)\cos[\Psi(t) + \Psi_0] \tag{2.17}$$

where

$$
\begin{aligned}
A(t) =& \sqrt{C_Q^2(t) + S_Q^2(t)} \\
\Psi(t) =& 2\Phi(t) - \arctan\left[\frac{S_Q(t)}{C_Q(t)}\right]
\end{aligned}
\tag{2.18}
$$

here, Ψ_0 is the constant initial phase that depends upon the initial configuration of the binary. In equation 2.18 we can see that the phase observed at the detector has an additional modulation which introduced by oscillatory nature of $C_Q(t)$ and $S_Q(t)$.

2.2 Detection of signals from inspiraling binaries

The GW signal $h(t, \boldsymbol{\lambda})$ observed by the detector is a function various parameters of the binary(i.e total mass,spins etc).In order to detect these signal we need to analyse the noisy interferometric data. For simplicity the noise $n(t)$ is assumed to be Gaussian with mean zero, characterized by its one sided power spectral density(PSD) $S_h(f)$. Noise is assumed to be additive, which means when signal is present in the data, then

$$d(t) = h(t; \boldsymbol{\lambda}) + n(t) \tag{2.19}$$

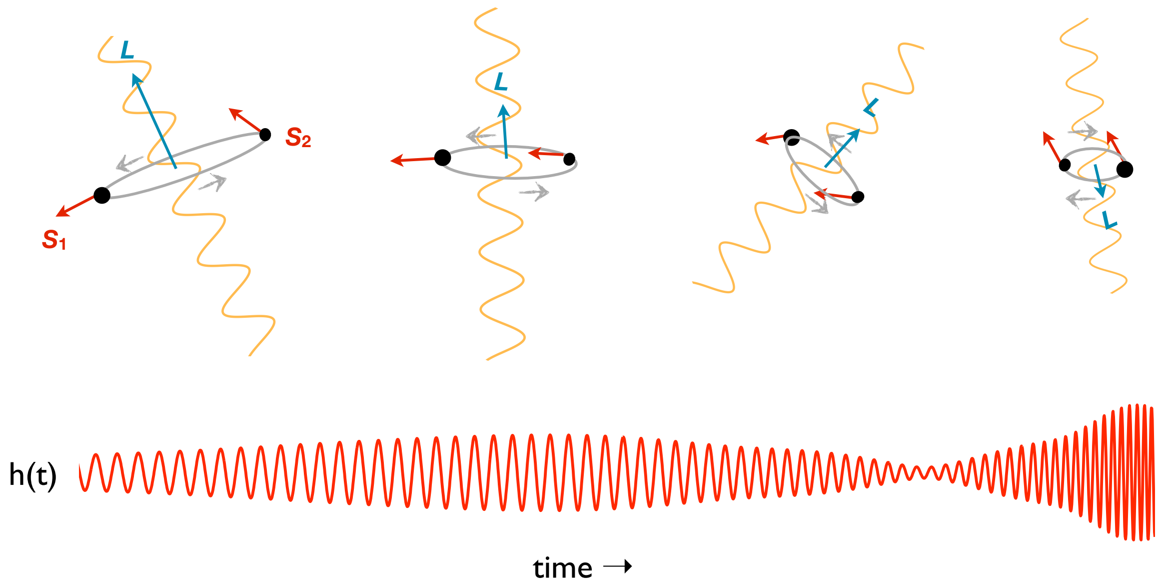

Figure 2.4: Above figure shows the time dependent waveform in detector's from observed from precessing binary black hole system

Under the additive assumption of detector noise, the Neyman-Pearson criteria gives an optimal search statistic. This when maximized over the overall amplitude of the signal, is the cross-correlation of the data with a normalized template.

$$\rho = \langle \hat{h}(\boldsymbol{\lambda}), d \rangle \tag{2.20}$$

here the normalized template is $\hat{h}(f) \equiv \tilde{h}(f)/\sqrt{\langle h, h \rangle}$. The angular bracket denotes the noise weighted inner product,called the overlap:

$$\langle a, b \rangle = 4\mathfrak{R} \int_{f_{low}}^{f_{cut}} df \frac{\tilde{a^*}(f)\tilde{b}(f)}{S_h(f)}, \tag{2.21}$$

here $\tilde{a}(f)$ and $\tilde{b}(f)$ are the Fourier transform of a(t) and b(t) respectively. Lower frequency cut off f_{low} is determined by the detector and the upper cut off f_{cut} is determined by the template waveform where the PN approximation breaks down.The optimal SNR is given by:

$$\rho_{opt} \equiv \langle h(\boldsymbol{\lambda}) h(\boldsymbol{\lambda}) \rangle^{1/2} \tag{2.22}$$

In a real search for a gravitational wave signal in detector data, where the binary parameter are not known a *priori*, it is required to maximize ρ over a "bank″ of templates corresponding to different values of parameter λ. The waveform also depends upon the arrival time t_0 of signal at the detector and the corresponding initial phase Ψ_0. The inner product in equation 2.21 between the template $x(\mathbf{\Lambda})$ and the target signal $h(\boldsymbol{\lambda})$ maximized over Ψ_0 and t_0 is called *match*:

$$\text{match} = \text{max}_{\Psi_0, t_0} \langle \hat{x}(\Psi_0, t_0, \Lambda), \hat{h}(\lambda) \rangle \tag{2.23}$$

A match maximized over all parameter of the template is called fitting factor:

$$\text{FF} = \text{max}_{\Psi_0, t_0, \mathbf{\Lambda}} \langle \hat{x}(\Psi_0, t_0, \Lambda), \hat{h}(\lambda) \rangle \tag{2.24}$$

Template families with high fitting factor(FF ≥ 0.97) are considered good for signal detection purpose and those with high value of match(match $\geq$ 0.97) are considered good for both signal detection and parameter estimations.

2.3 Computing ovrlaps

The inner product in equation 2.21 requires modelling of the PSD of the detector noise. The expected PSD of the Advanced LIGO has the following functional form:

$$\begin{aligned} S_h(f) = & 10^{-48}(0.0152x^{-4} + 0.2935x^{9/4} + 2.7951x^{3/2} - 6.5080x^{3/4} \\ & + 17.7622), \end{aligned} \tag{2.25}$$

where x = f/245.4. The lower cut off frequency for Advanced LIGO is assumed to be 20 Hz. The upper cut off is chosen as the radius of inner most stable orbit(ISCO) of a test particle in an orbit around schwarzschild black hole.$f_{\text{ISCO}} = v^3/(\pi m)$, where $v_{\text{ISCO}=1/\sqrt{6}}$.

2.4 Fourier domain templates for inspiralling binaries with generic spins

In case of binaries with spins that are neither aligned nor anti aligned with orbital angular momentum, the spins and orbital angular momentum evolves according to equation 2.7 and 2.8. The cross correlation between the data and the template is most efficiently computed in Fourier domain.For the case of precessing binaries we try to obtain the Fourier domain waveform in a semi- analytical way using stationary phase approximation.

2.4.1 Fourier transform using stationary phase approximation

If a given time domain signal obeys certain mathematical properties, then the Fourier transform can be computed in a way which simplifies the integration involved in taking Fourier transform. Let us consider a time domain signal:

$$\begin{aligned} h(t) =& 2a(t)\cos\phi(t) = a(t)\, e^{-i\phi} + a(t)\, e^{i\phi} \\ \text{where, } \frac{d\phi}{dt} \equiv& 2\pi \mathrm{F}(t) > 0. \end{aligned} \tag{2.26}$$

The Fourier transform (FT) $\tilde{h}(f)$ of a time-domain signal $h(t)$ is given by:

$$h(t) = \int_{-\infty}^{\infty} df\, e^{-2\pi i f t}\tilde{h}(f); \quad \tilde{h}(f) = \int_{-\infty}^{\infty} dt\, e^{2\pi i f t} h(t) \tag{2.27}$$

In equation equation 2.26 , the signal $h(t)$ is real.For a real signal we an identity $\tilde{h}(f) \equiv (\tilde{h}(-f))^*$. It is therefore suffice to compute the Fourier transform for positive valves of the frequency f. We can write equation 2.26 in the following way:

$$\tilde{h}(f) = \tilde{h}_-(f) + \tilde{h}_+(f) \tag{2.28a}$$

$$\text{where, } \tilde{h}_-(f) \equiv \int_{-\infty}^{\infty} dt\, a(t) e^{i(2\pi f t - \phi(t))} \tag{2.28b}$$

$$\tilde{h}_+(f) \equiv \int_{-\infty}^{\infty} dt\, a(t) e^{i(2\pi f t + \phi(t))} \tag{2.28c}$$

The integrands of $\tilde{h}_\pm(f)$ are violently oscillating and thus their dominant contribution come from the vicinity of the stationary points of their phase(when such point exits). When $f > 0$, it can be seen that only $\tilde{h}_-(f)$ term has such a saddle point. Therefore, we can write the approximation

$$\tilde{h}(f) \simeq \tilde{h}_-(f) \simeq \int_{-\infty}^{\infty} dt\, a(t)\, e^{i\psi_f(t)} \tag{2.29a}$$

$$\text{where, } \psi_f(t) \equiv 2\pi f t - \phi(t) \tag{2.29b}$$

The saddle-point of the phase $\psi_f(t)$ is the value, say t_f of the time variable where $d\psi_f(t)/dt = 0$. It is the solution of the equation $F(t_f) = f$. The dominant contribution to the integral equation 2.28a comes from the time interval t near t_f.Taylor expansion of the phase and amplitude near the saddle point t_f and truncation at quadratic and linear order for phase and amplitude respectively leads to the following equations

$$\psi_f(t) \simeq \psi_f(t_f) - \pi \dot{F}(t_f)(t - t_f)^2 \tag{2.30a}$$

$$a(t) \simeq a(t_f) \tag{2.30b}$$

The first order term in amplitude vanish after integration in the above equation, so we keep zeroth order term in amplitude. This leads to a Gaussian integral

$$\tilde{h}(f) \simeq \int_{-\infty}^{\infty} dt\, a(t_f)\, e^{i\psi_f(t_f) - i\pi \dot{F}(t_f)(t-t_f)^2} \tag{2.31}$$

Above equation is a standard well know Gaussian integral which on integration gives the following result.

$$\tilde{h}(f)^{uspa} = \frac{a(t_f)}{\sqrt{\dot{F}(t_f)}}\, e^{[\psi_f(t_f) - \pi/4]} \tag{2.32}$$

In the above equation uspa denotes usual stationary phase approximation. Here $\psi_f(t_f)$ is the value of $\psi_f(t)$ at $t = t_f$. The mathematical condition for the validity of the SPA are usually assumed to be $\epsilon_1 \ll 1$ and $\epsilon_2 \ll 1$, where

$$\epsilon_1 \equiv \left| \frac{\dot{a(t)}}{a(t)\dot{\phi(t)}} \right|; \;\; \epsilon_2 \equiv \left| \frac{\ddot{\phi}(t)}{\dot{\phi}^2(t)} \right| = \left| \frac{1}{2\pi} \frac{\dot{F}(t)}{F^2(t)} \right| \tag{2.33}$$

Chapter 3

Construction of Fourier domain waveform for gravitational waves from binary black holes with generic spins

3.1 COMPUTING THE SPIN AND ANGULAR MOMENTUM VECTORS IN THE FREQUENCY DOMAIN

The spin angular momentum vector $\boldsymbol{S}_i(v)$ and the unit vector $\hat{\boldsymbol{L}}_N(v)$ along the Newtonian angular momentum in frequency domain can be computed by using the evolution equation.

$$\frac{d\boldsymbol{S}_i}{dv} = \frac{d\boldsymbol{S}_i}{dt}\frac{dt}{dv} \tag{3.1}$$

$$\frac{d\hat{\boldsymbol{L}}_N}{dv} = \frac{d\hat{\boldsymbol{L}}_N}{dt}\frac{dt}{dv} \tag{3.2}$$

where

$$\frac{d\hat{\boldsymbol{L}}_N}{dt} = -\frac{1}{\|L\|}\frac{d}{dt}(\boldsymbol{S}_1 + \boldsymbol{S}_2) \tag{3.3}$$

$$\frac{d\boldsymbol{S}_i}{dt} = \boldsymbol{\Omega_i} \times \boldsymbol{S}_i,\ i = 1, 2, \tag{3.4}$$

$$\frac{dt}{dv} = \frac{-mE'(v)}{\mathcal{F}(v)} \tag{3.5}$$

The explicit expressions for $-E'(v)/\mathcal{F}(v)$, $\mathbf{\Omega}_1$ and $\mathbf{\Omega}_2$ are given in equation 2.3, 2.8 and 2.7 respectively. These coupled equations are solved numerically with appropriate initial conditions. The initial conditions for the ODEs correspond to the initial configurations of binary with respect to the coordinate system described in Fig. 2.1

3.2 COMPUTATION OF THE FOURIER TRANSFORM USING STATIONARY PHASE APPROXIMATION

We have the spin vector $\boldsymbol{\chi_1}(v)$ and $\boldsymbol{\chi_2}(v)$, and the orbital angular momentum(unit) vector $\hat{\boldsymbol{L}}_N(v)$ as a function of v.Using these inputs the Fourier transform of the two polarization component in the source frame using stationary phase approximation is given by

$$\tilde{h}_{+,\times}(f,\boldsymbol{\chi_1}(f),\boldsymbol{\chi_2}(f)) = A_{+,\times}(f,\boldsymbol{\chi_1}(f),\boldsymbol{\chi_2}(f))e^{i\Psi_{+,\times}(f,\boldsymbol{\chi_1}(f),\boldsymbol{\chi_2}(f))} \tag{3.6}$$

where

$$A_{+,\times}(f,\boldsymbol{\chi_1}(f),\boldsymbol{\chi_2}(f)) = \frac{\sqrt{C^2_{+,\times}(v_f)+S^2_{+,\times}(v_f)}}{2}\left[\frac{dF(v_f)}{dt}\right]^{-1/2} \tag{3.7}$$

where $v_f = (\pi m f)^{1/3}$, $F(v_f) = v_f^3/(\pi m) \; - (d\alpha/dt)\cos i$ is the instantaneous GW frequency(of the dominant harmonic) evaluated at the stationary point v_f. α and i are the angles describing the evolution of the orbital angular momentum vector $\hat{\boldsymbol{L}}_N$ in the Finn-Chernoff co-ordinate system as explained in equation 2.12.t_0 is the arrival time of the signal at the detector, Ψ_0 is the corresponding initial phase and

$$
\begin{aligned}
\Psi(f) =& \frac{3}{128\eta v^5}\Bigg\{1 + v^5\left[\frac{55\eta}{9} + \frac{3715}{756}\right] + v^3[4\beta - 16\pi] + \\
& v^4\left[\frac{3085\eta^2}{72} + \frac{27145\eta}{504} + \frac{15293365}{508032} - 10\sigma\right] + \\
& v^5\left[\frac{38645\pi}{756} - \frac{65\eta\pi}{9} - \gamma\right](3\ln(v) + 1) + v^6\Bigg[-\frac{6848\gamma_E}{21} - \frac{127825\eta^3}{1296} \\
& + \frac{76055\eta^2}{1728} + \left(\frac{2255\pi^2}{12} - \frac{15737765635}{3048192}\right)\eta - \frac{640\pi^2}{3} + \frac{11583231236531}{4694215680} \\
& - \frac{6848\ln(4v)}{21}\Bigg] + v^7\left[-\frac{74045\pi\eta^2}{756} + \frac{378515\eta\pi}{1512} + \frac{77096675\pi}{254016}\right]
\end{aligned}
\tag{3.8}
$$

where the terms

$$
\begin{aligned}
\beta =& \frac{113}{12}\left(\chi_s + \delta\chi_a - \frac{76\eta}{113}\chi_s\right), \\
\sigma =& \chi_a^2\left(\frac{81}{16} - 20\eta\right) + \frac{81\chi_a\chi_s\delta}{8} + \chi_s^2\left(\frac{81}{16} - \frac{\eta}{4}\right), \\
\gamma =& \chi_a\delta\left(\frac{140\eta}{9} + \frac{732985}{2268}\right) + \chi_s\left(\frac{732985}{2268} - \frac{24260\eta}{81} - \frac{340\eta^2}{9}\right),
\end{aligned}
\tag{3.9}
$$

denote the leading-order spin-orbit coupling, leading-order spin-spin coupling, and the next-to-leading-order spin-order coupling, respectively.

The time-derivative of the GW frequency appearing in equation 3.7 can be written as:

$$
\frac{dF(v_f)}{dt} = \frac{dF}{dv_f}\frac{dv_f}{dE}\frac{dE}{dt} = \frac{3v_f^2}{\pi m^2}\left[\frac{-\mathcal{F}(v_f)}{E'(v_f}\right] \tag{3.10}
$$

where we use the energy balance equation $mdE/dt = -\mathcal{F}(v)$, and the definition $E'(v) \equiv dE/dv$. This can be plugged back to Equation 3.7 to get a closed form expression of A(f).

$$
A_{+,\times}(f, \boldsymbol{\chi_1}(f), \boldsymbol{\chi_2}(f)) = \frac{m\sqrt{C_{+,\times}^2(v_f) + S_{+,\times}^2(v_f)}}{2v_f}\sqrt{\frac{\pi}{3}}\left[\frac{-E'(v_f)}{\mathcal{F}(v_f)}\right] \tag{3.11}
$$

In the expression above we use the expansion of $-E'(v_f/\mathcal{F}(v_f)$ as given in equation 2.3.

Chapter 4

Results

4.1 Numerical results of Fourier transform using SPA and comparison with numerical FFT

In our calculation of Fourier domain template, we use several approximations.These approximations include,
1. For the calculation of Fourier frequency we neglect contribution coming due to effect precession.

$$i.e. \qquad 2\pi f = \frac{d\Phi}{dt} = \frac{v^3}{M} - \frac{d\alpha}{dt}\cos i \approx \frac{v^3}{M} \tag{4.1}$$

In the above equation we neglect the contribution of $(d\alpha/dt)\cos i$
2. We neglect the contribution coming due to precessing effect in phase of SPA formula.

$$\Phi(t_f) = \int_{t_0}^{t_f} \Big(\frac{v^3}{M} - \frac{d\alpha}{dt}\cos i\Big) dt \approx \int_{t_0}^{t_f} \frac{v^3}{M} dt \tag{4.2}$$

The complete phase in SPA is given by $\Psi_f(f) = 2\pi f t_f - 2\Phi(t_f)$

We plot the Fourier domain waveform for different mass ratios, with different spin configuration of binary in source frame and angle between the line of sight from the detector to the source and the z-axis of the coordinate system

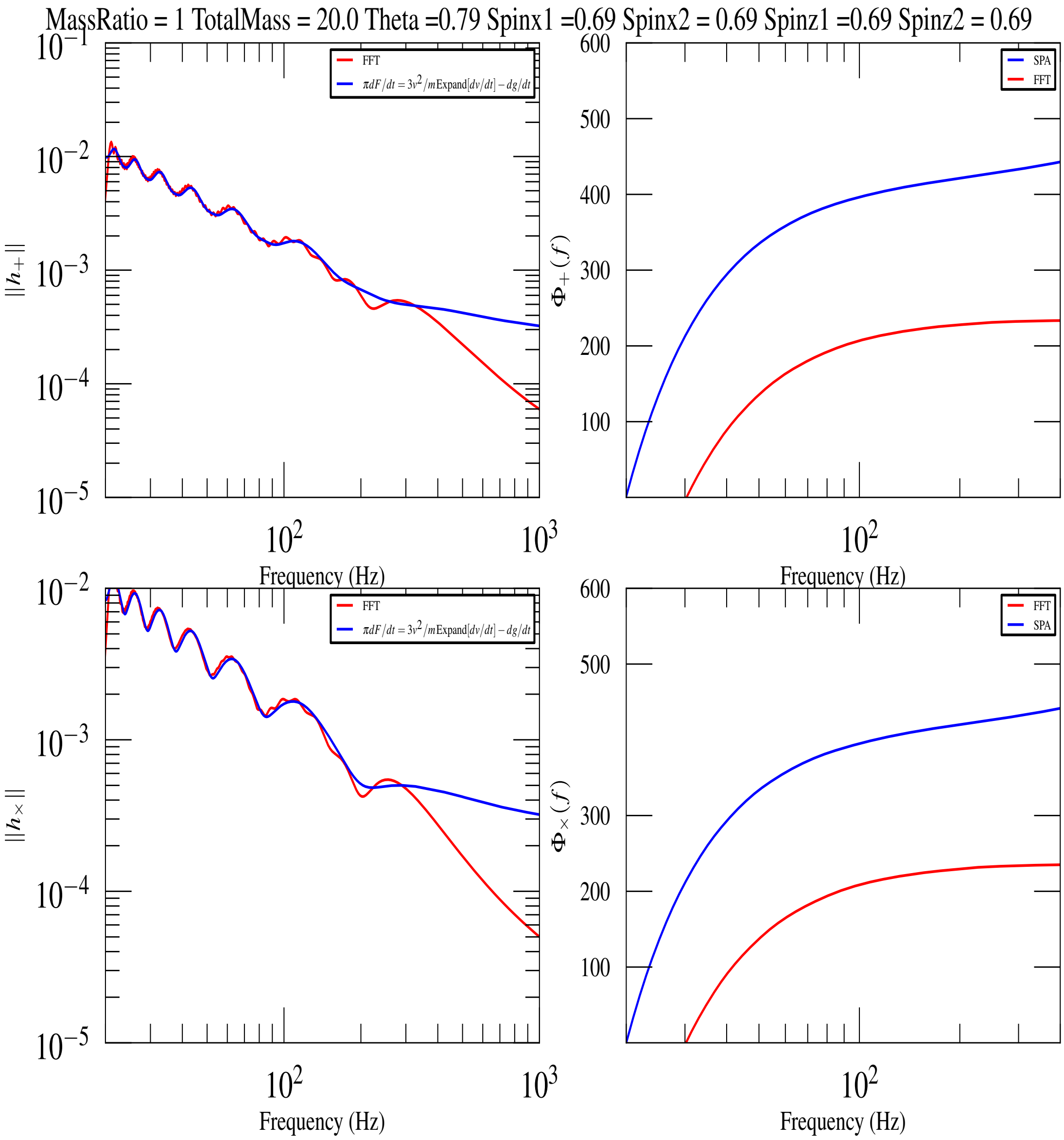

Figure 4.1: Above figure shows the Fourier domain gravitational waveform from binary balck hole system with the parameters mentioned on the top .In the above figure the left column shows the comparison of the amplitude of two polarization($h_+(v)$ and $h_\times(v)$) in Fourier domain, obtained using stationary phase approximation and numerical FFT. The right column shows a similar comparison for phase for the two polarization components.

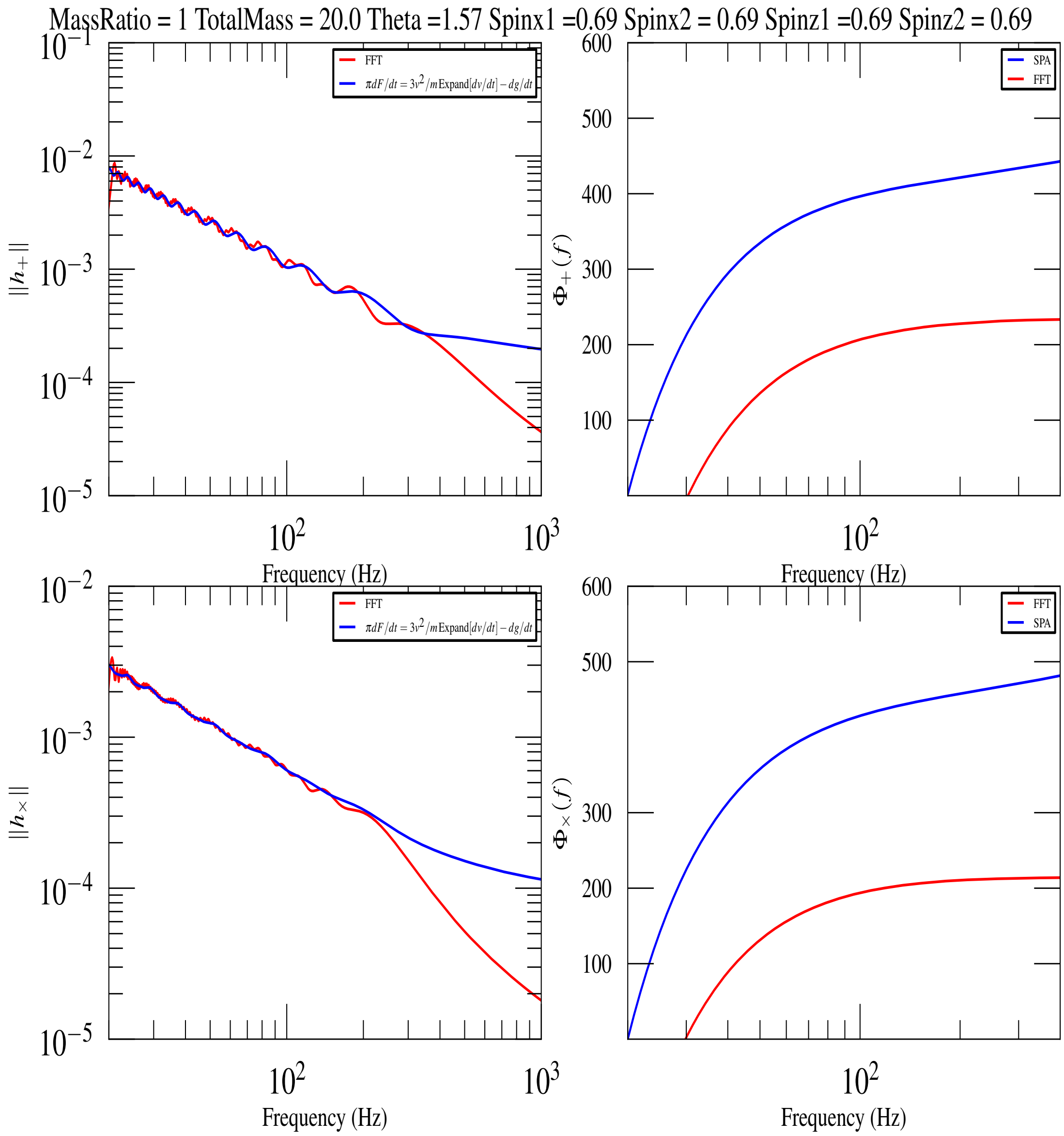

Figure 4.2: Above figure shows the Fourier domain gravitational waveform from binary balck hole system with the parameters mentioned on the top .In the above figure the left column shows the comparison of the amplitude of two polarization($h_+(v)$ and $h_\times(v)$) in Fourier domain, obtained using stationary phase approximation and numerical FFT. The right column shows a similar comparison for phase for the two polarization components.

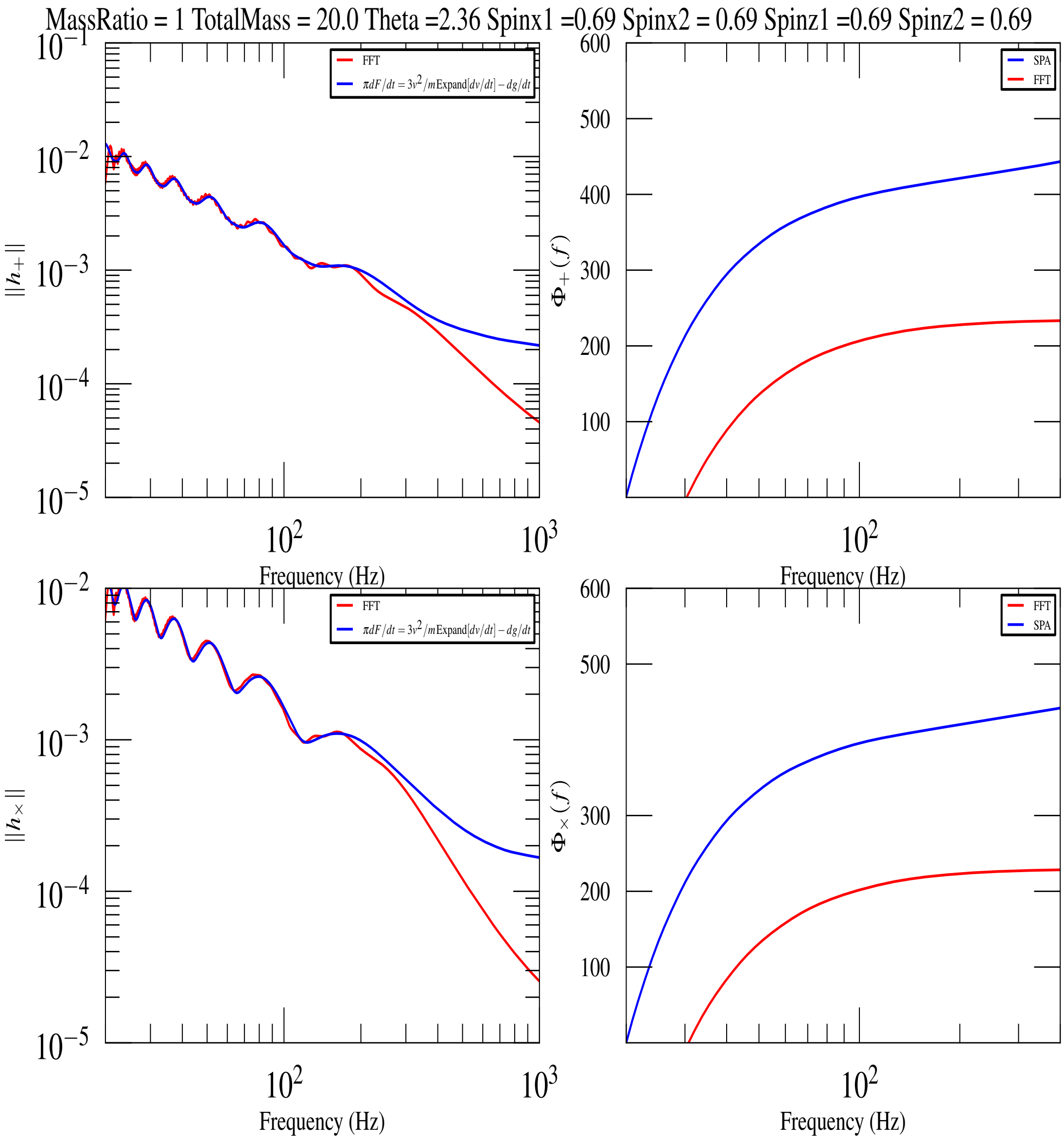

Figure 4.3: Above figure shows the Fourier domain gravitational waveform from binary balck hole system with the parameters mentioned on the top .In the above figure the left column shows the comparison of the amplitude of two polarization($h_+(v)$ and $h_\times(v)$) in Fourier domain, obtained using stationary phase approximation and numerical FFT. The right column shows a similar comparison for phase for the two polarization components.

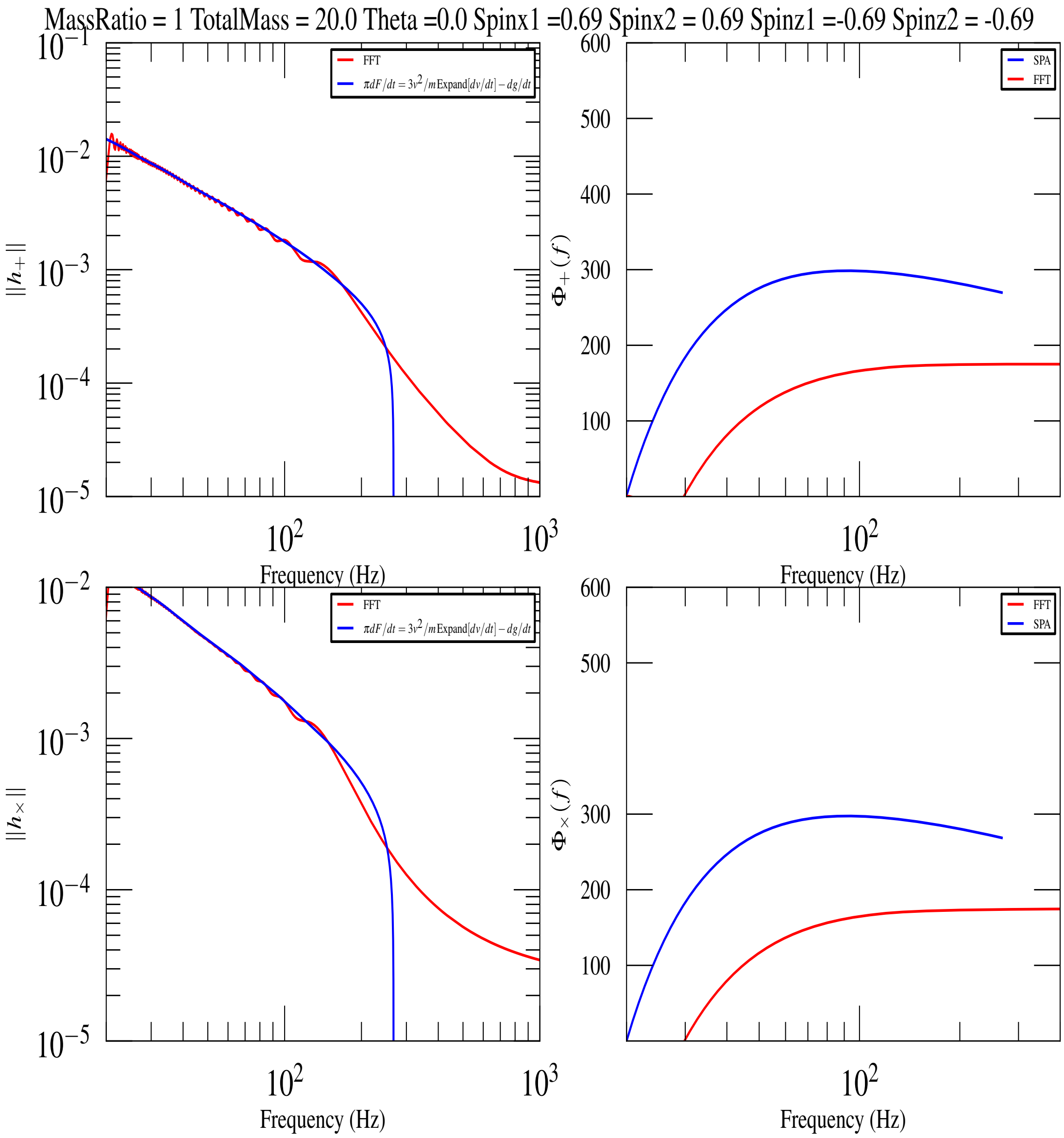

Figure 4.4: Above figure shows the Fourier domain gravitational waveform from binary balck hole system with the parameters mentioned on the top .In the above figure the left column shows the comparison of the amplitude of two polarization($h_+(v)$ and $h_\times(v)$) in Fourier domain, obtained using stationary phase approximation and numerical FFT. The right column shows a similar comparison for phase for the two polarization components.

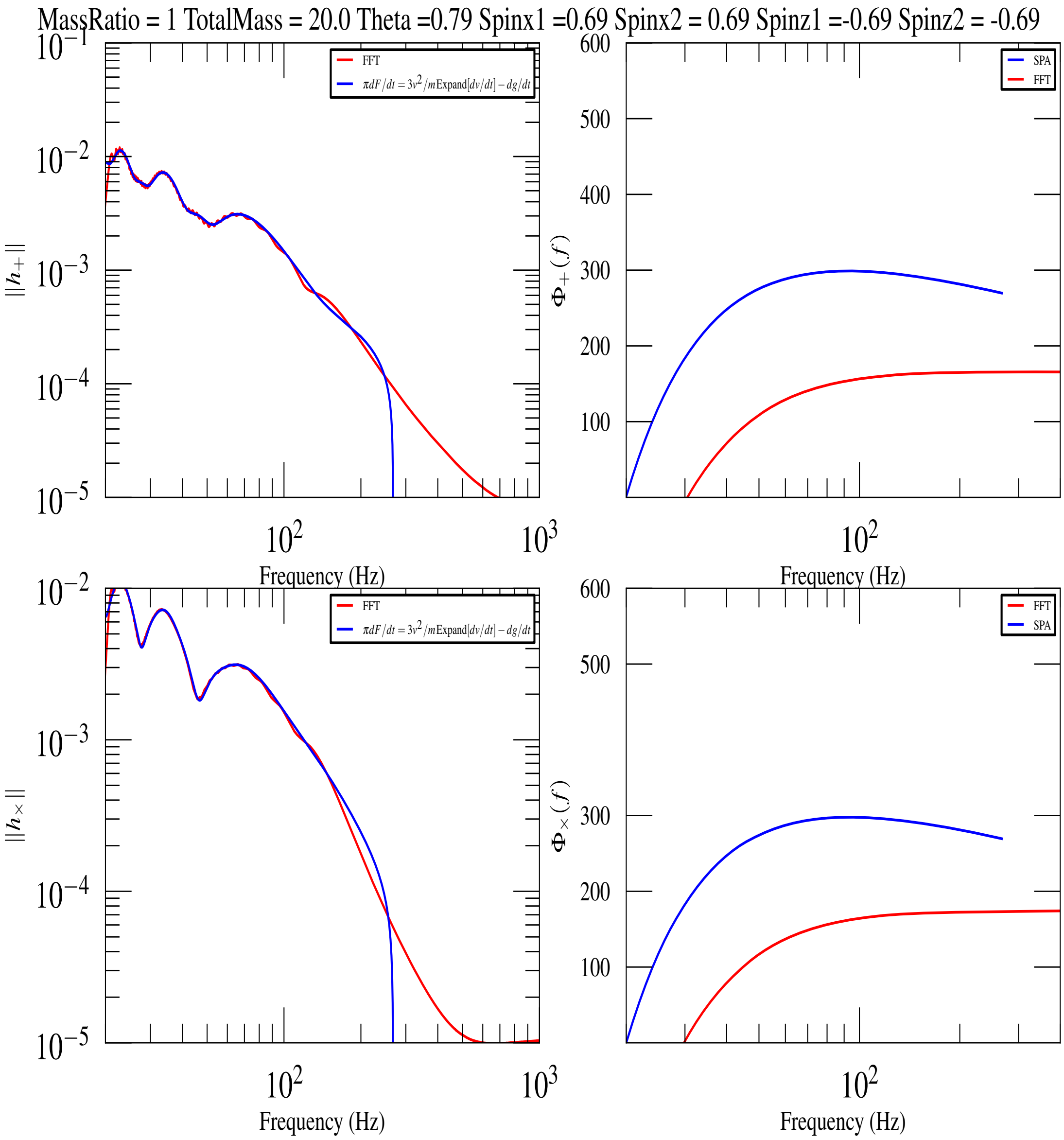

Figure 4.5: Above figure shows the Fourier domain gravitational waveform from binary balck hole system with the parameters mentioned on the top .In the above figure the left column shows the comparison of the amplitude of two polarization($h_+(v)$ and $h_\times(v)$) in Fourier domain, obtained using stationary phase approximation and numerical FFT. The right column shows a similar comparison for phase for the two polarization components.

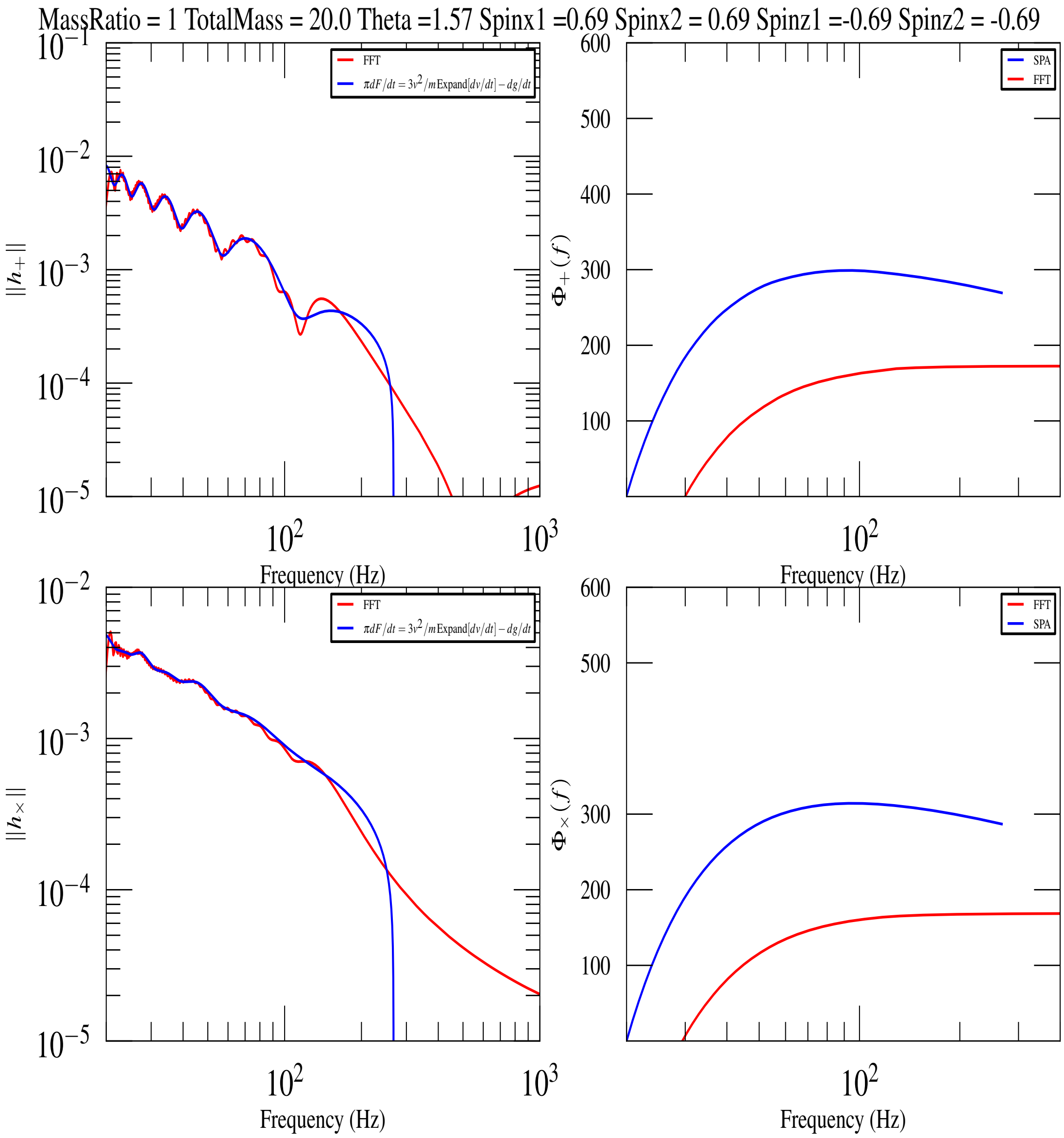

Figure 4.6: Above figure shows the Fourier domain gravitational waveform from binary balck hole system with the parameters mentioned on the top .In the above figure the left column shows the comparison of the amplitude of two polarization($h_+(v)$ and $h_\times(v)$) in Fourier domain, obtained using stationary phase approximation and numerical FFT. The right column shows a similar comparison for phase for the two polarization components.

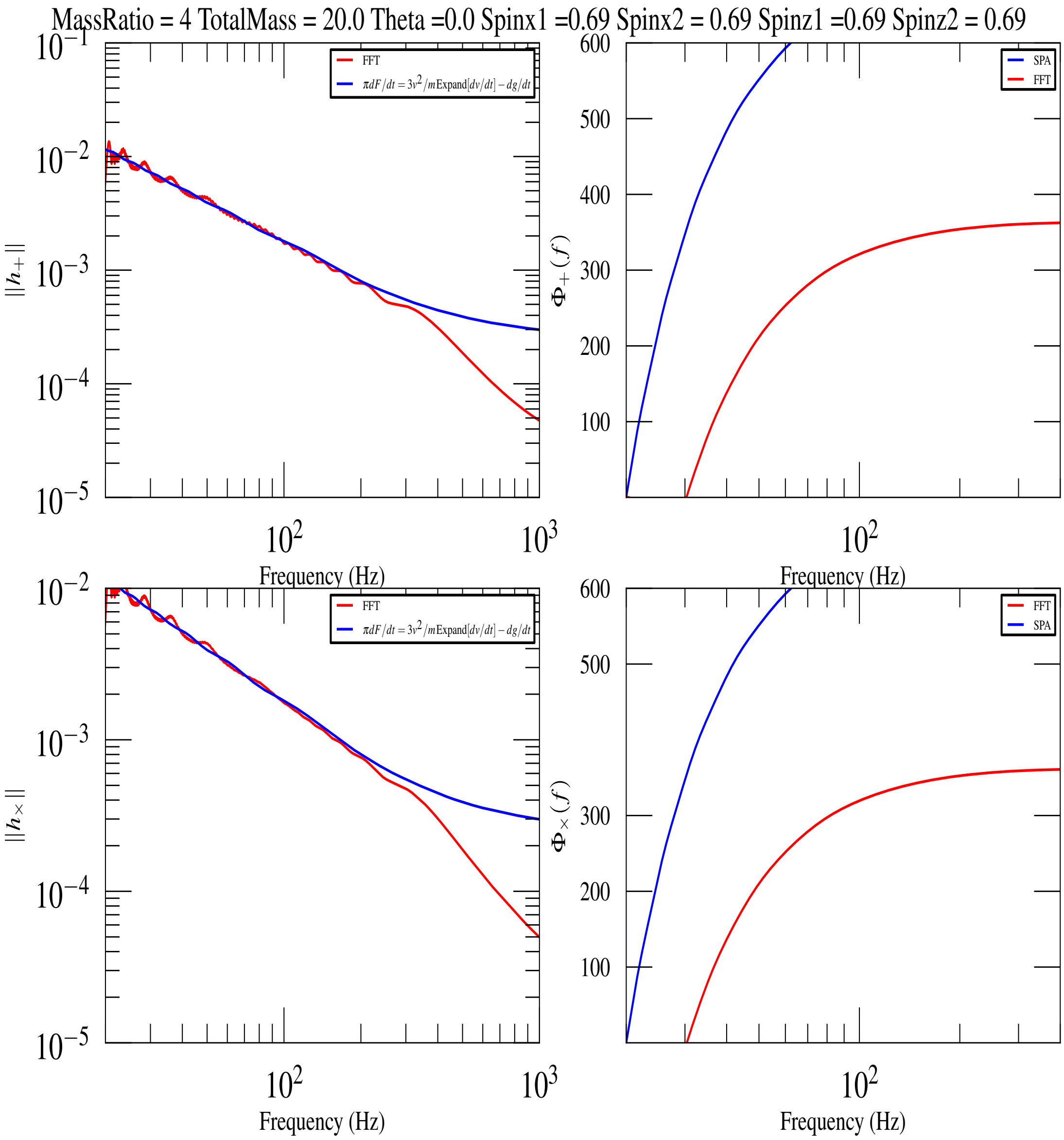

Figure 4.7: Above figure shows the Fourier domain gravitational waveform from binary balck hole system with the parameters mentioned on the top .In the above figure the left column shows the comparison of the amplitude of two polarization($h_+(v)$ and $h_\times(v)$) in Fourier domain, obtained using stationary phase approximation and numerical FFT. The right column shows a similar comparison for phase for the two polarization components.

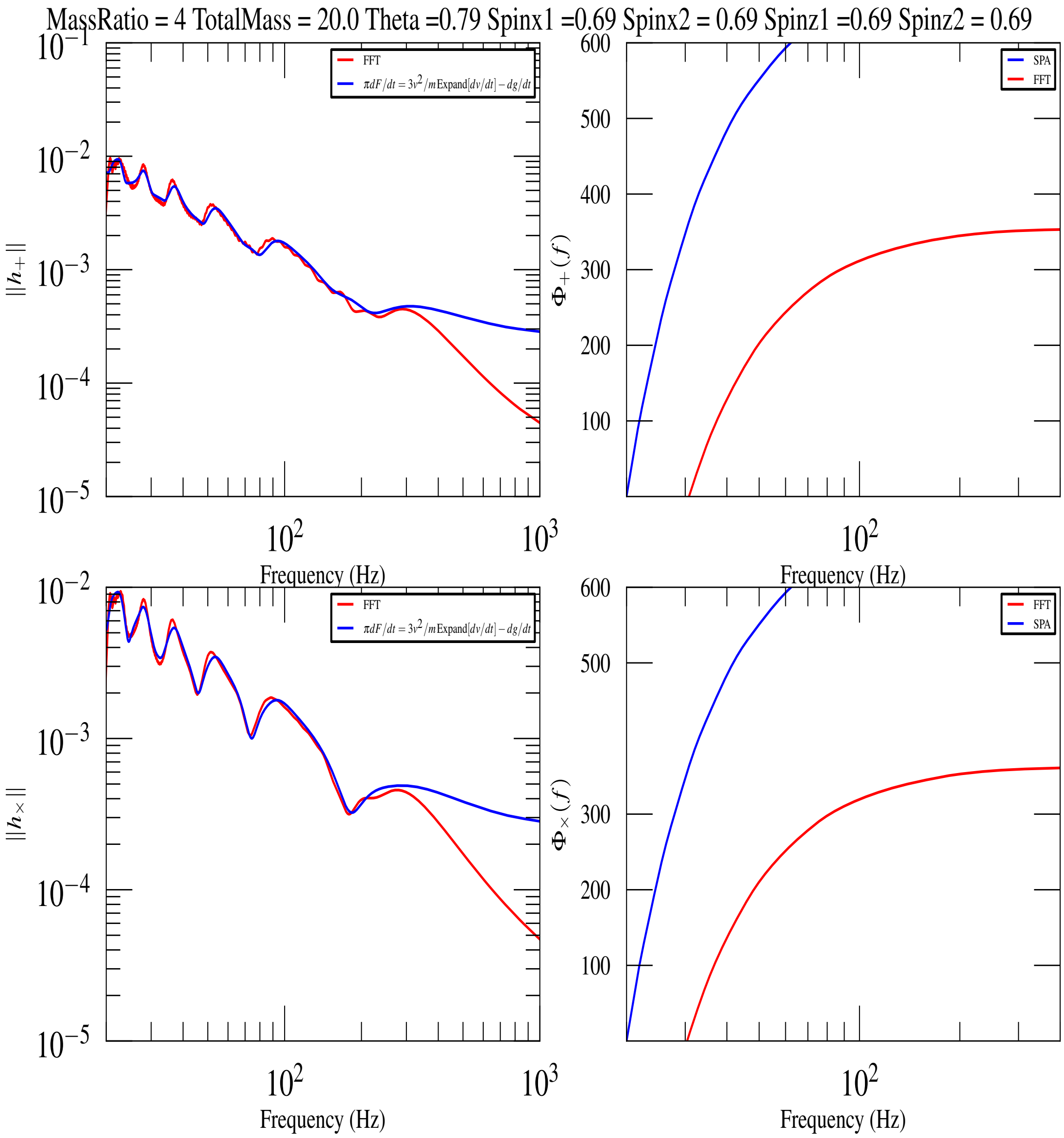

Figure 4.8: Above figure shows the Fourier domain gravitational waveform from binary balck hole system with the parameters mentioned on the top .In the above figure the left column shows the comparison of the amplitude of two polarization($h_+(v)$ and $h_\times(v)$) in Fourier domain, obtained using stationary phase approximation and numerical FFT. The right column shows a similar comparison for phase for the two polarization components.

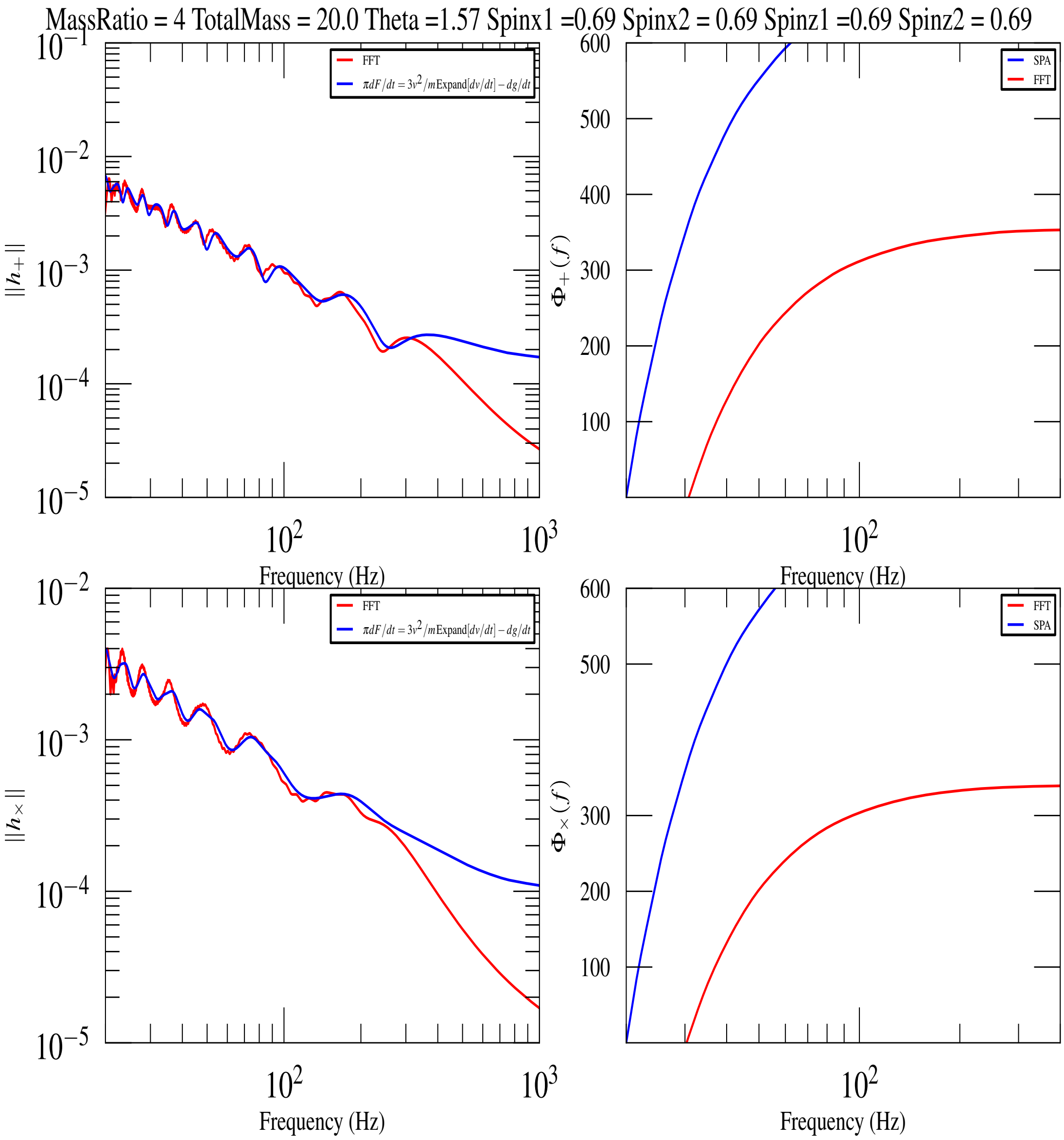

Figure 4.9: Above figure shows the Fourier domain gravitational waveform from binary balck hole system with the parameters mentioned on the top .In the above figure the left column shows the comparison of the amplitude of two polarization($h_+(v)$ and $h_\times(v)$) in Fourier domain, obtained using stationary phase approximation and numerical FFT. The right column shows a similar comparison for phase for the two polarization components.

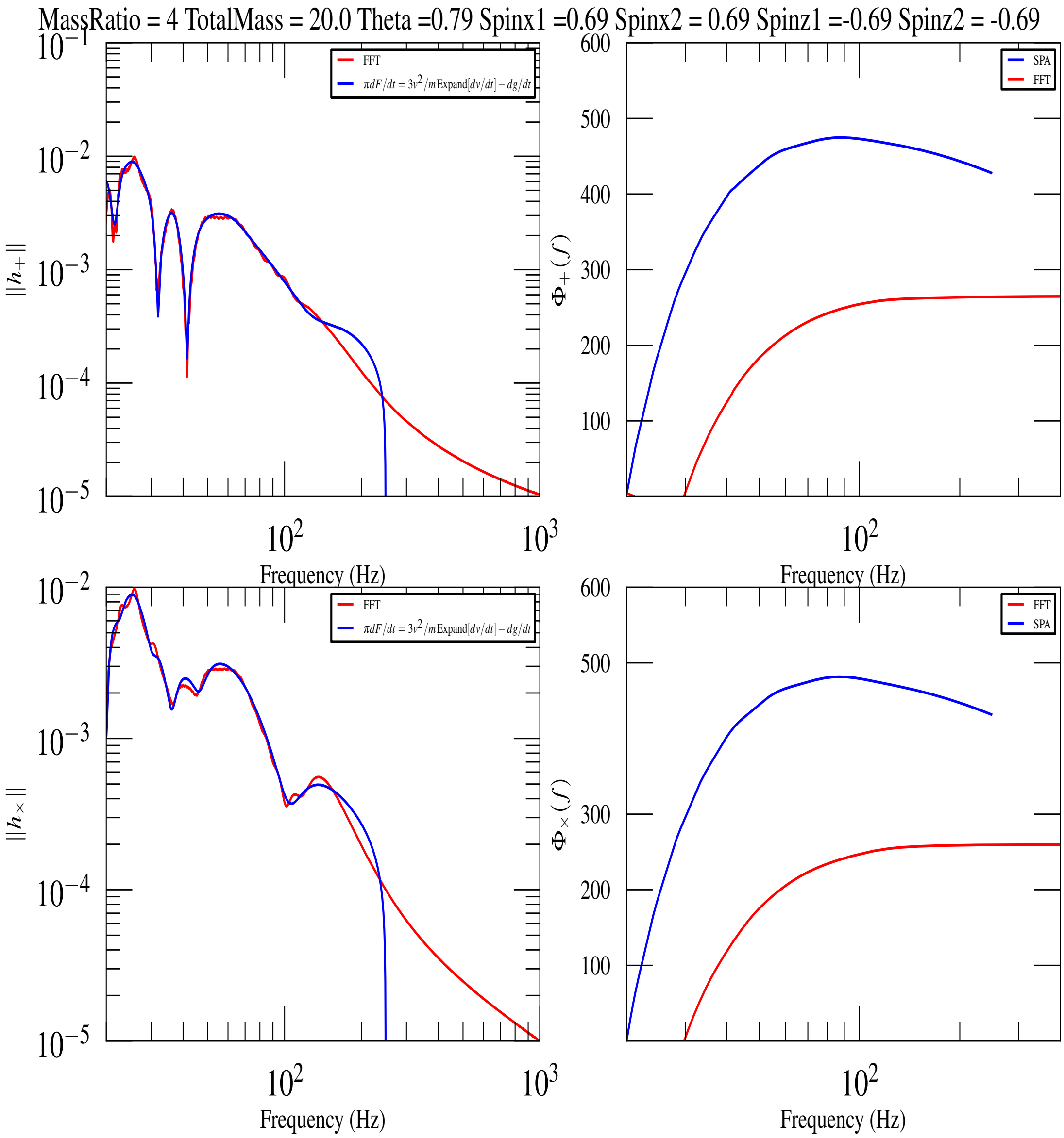

Figure 4.10: Above figure shows the Fourier domain gravitational waveform from binary balck hole system with the parameters mentioned on the top .In the above figure the left column shows the comparison of the amplitude of two polarization($h_+(v)$ and $h_\times(v)$) in Fourier domain, obtained using stationary phase approximation and numerical FFT. The right column shows a similar comparison for phase for the two polarization components.

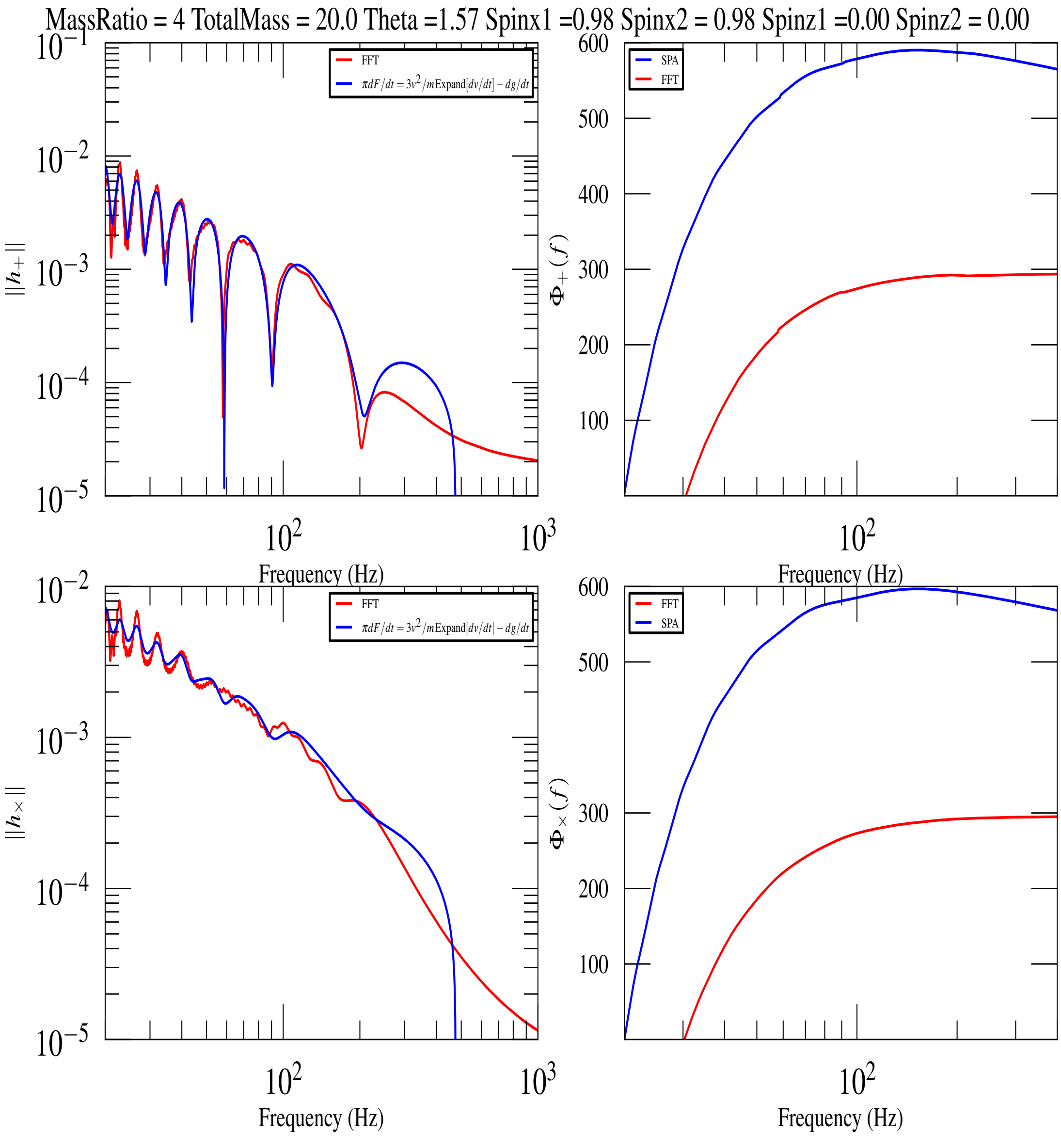

Figure 4.11: Above figure shows the Fourier domain gravitational waveform from binary balck hole system with the parameters mentioned on the top .In the above figure the left column shows the comparison of the amplitude of two polarization($h_+(v)$ and $h_\times(v)$) in Fourier domain, obtained using stationary phase approximation and numerical FFT. The right column shows a similar comparison for phase for the two polarization components.

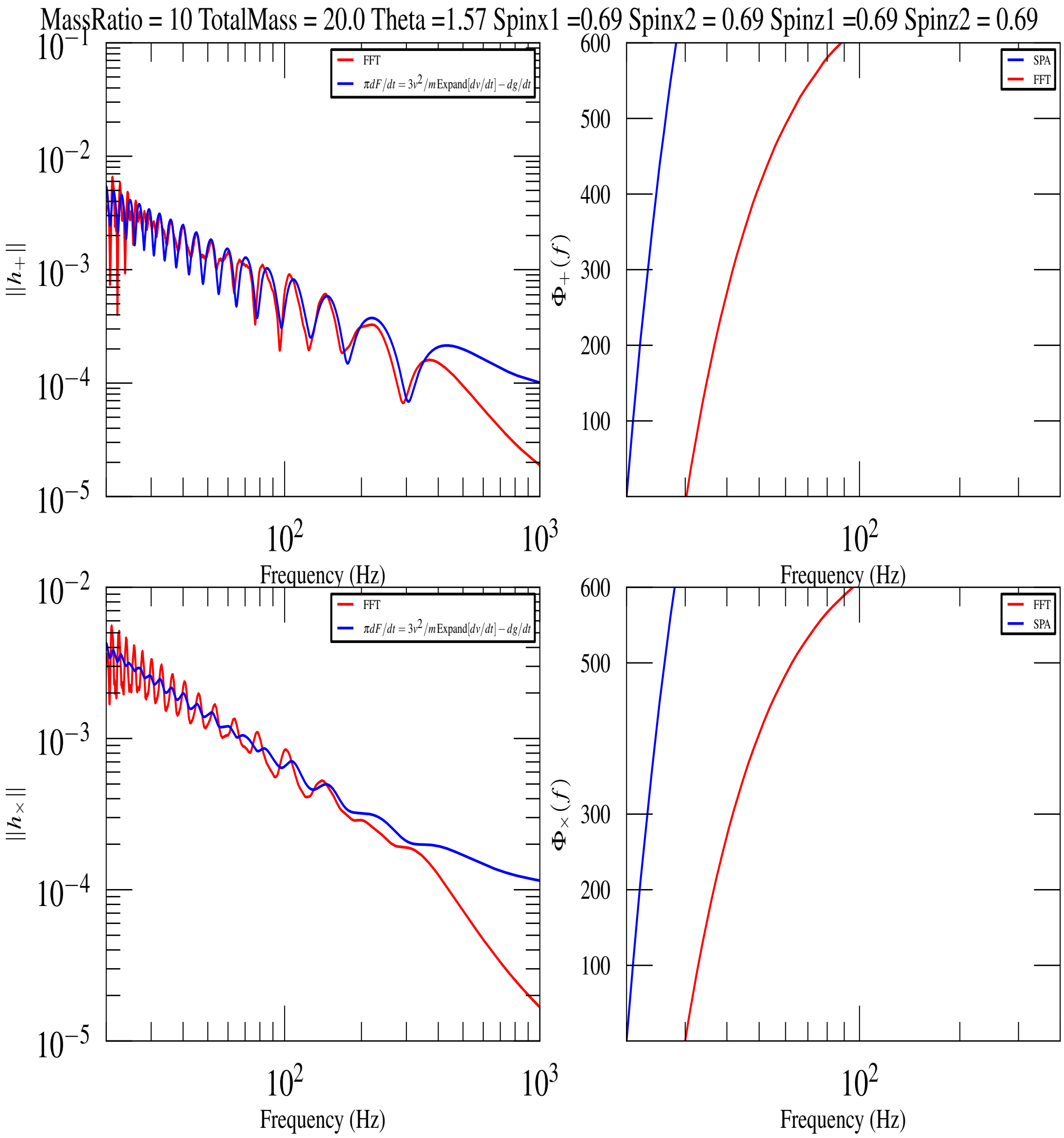

Figure 4.12: Above figure shows the Fourier domain gravitational waveform from binary balck hole system with the parameters mentioned on the top .In the above figure the left column shows the comparison of the amplitude of two polarization($h_+(v)$ and $h_\times(v)$) in Fourier domain, obtained using stationary phase approximation and numerical FFT. The right column shows a similar comparison for phase for the two polarization components.

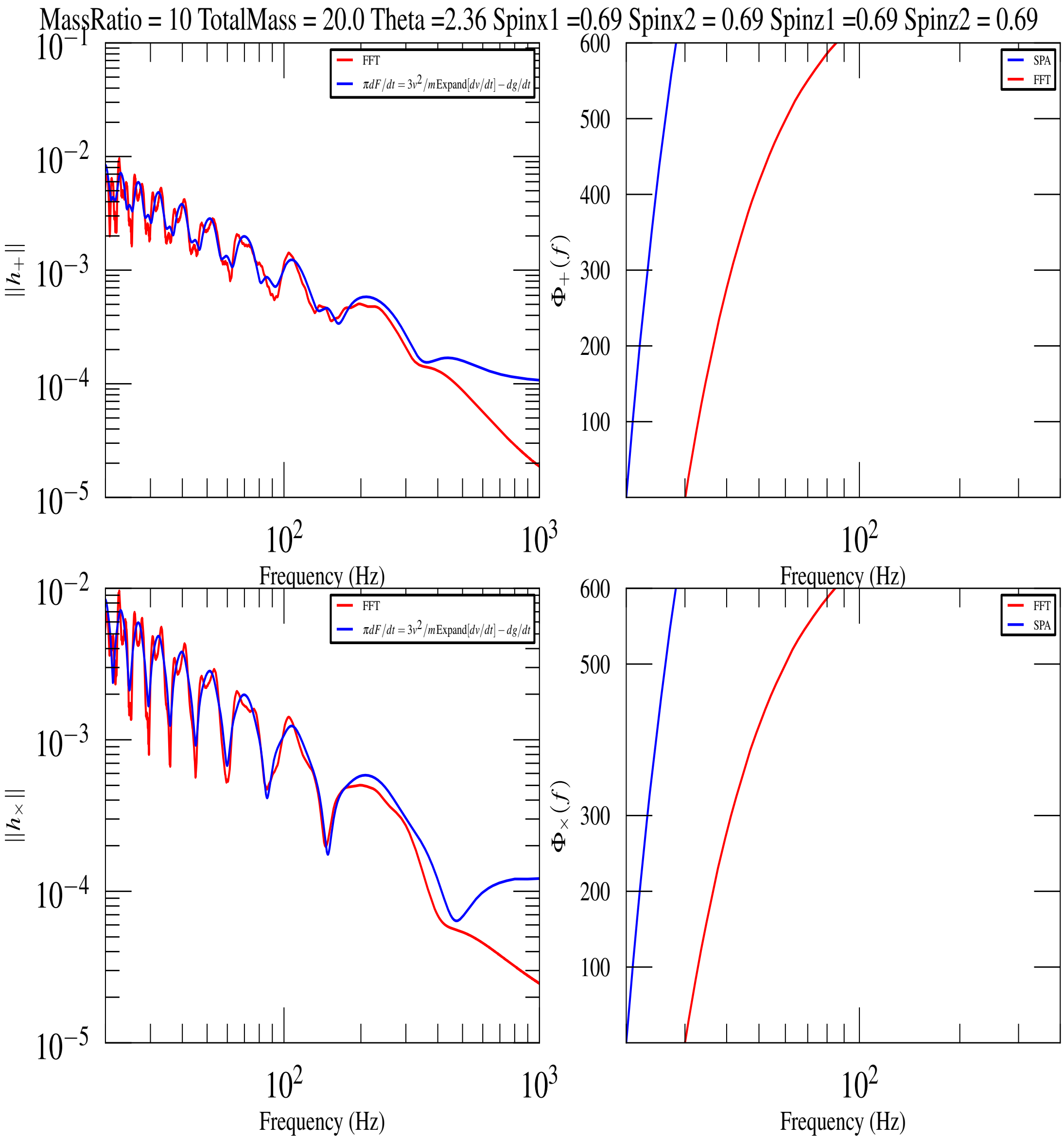

Figure 4.13: Above figure shows the Fourier domain gravitational waveform from binary balck hole system with the parameters mentioned on the top .In the above figure the left column shows the comparison of the amplitude of two polarization($h_+(v)$ and $h_\times(v)$) in Fourier domain, obtained using stationary phase approximation and numerical FFT. The right column shows a similar comparison for phase for the two polarization components.

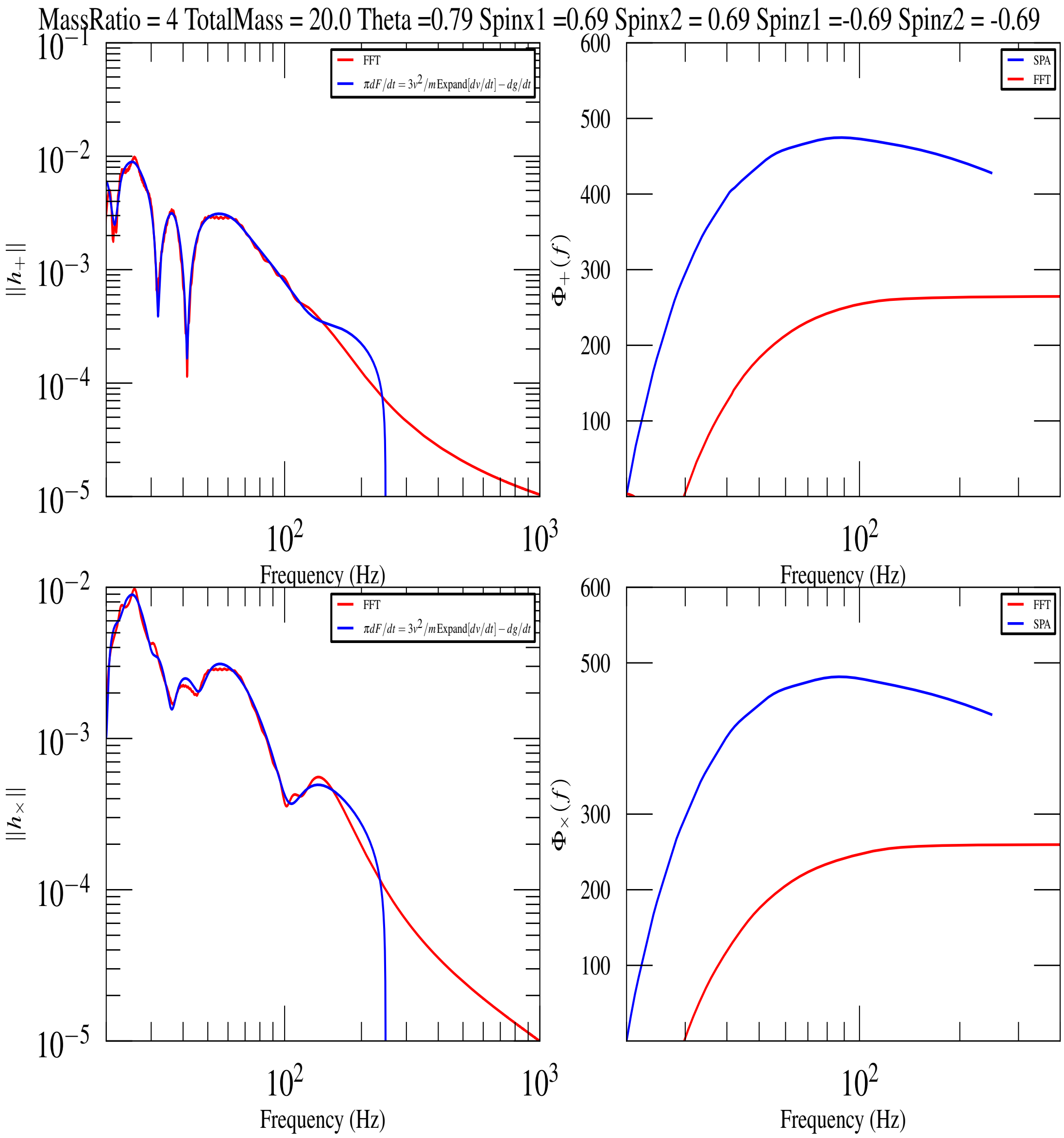

Figure 4.14: Above figure shows the Fourier domain gravitational waveform from binary balck hole system with the parameters mentioned on the top .In the above figure the left column shows the comparison of the amplitude of two polarization($h_+(v)$ and $h_\times(v)$) in Fourier domain, obtained using stationary phase approximation and numerical FFT. The right column shows a similar comparison for phase for the two polarization components.

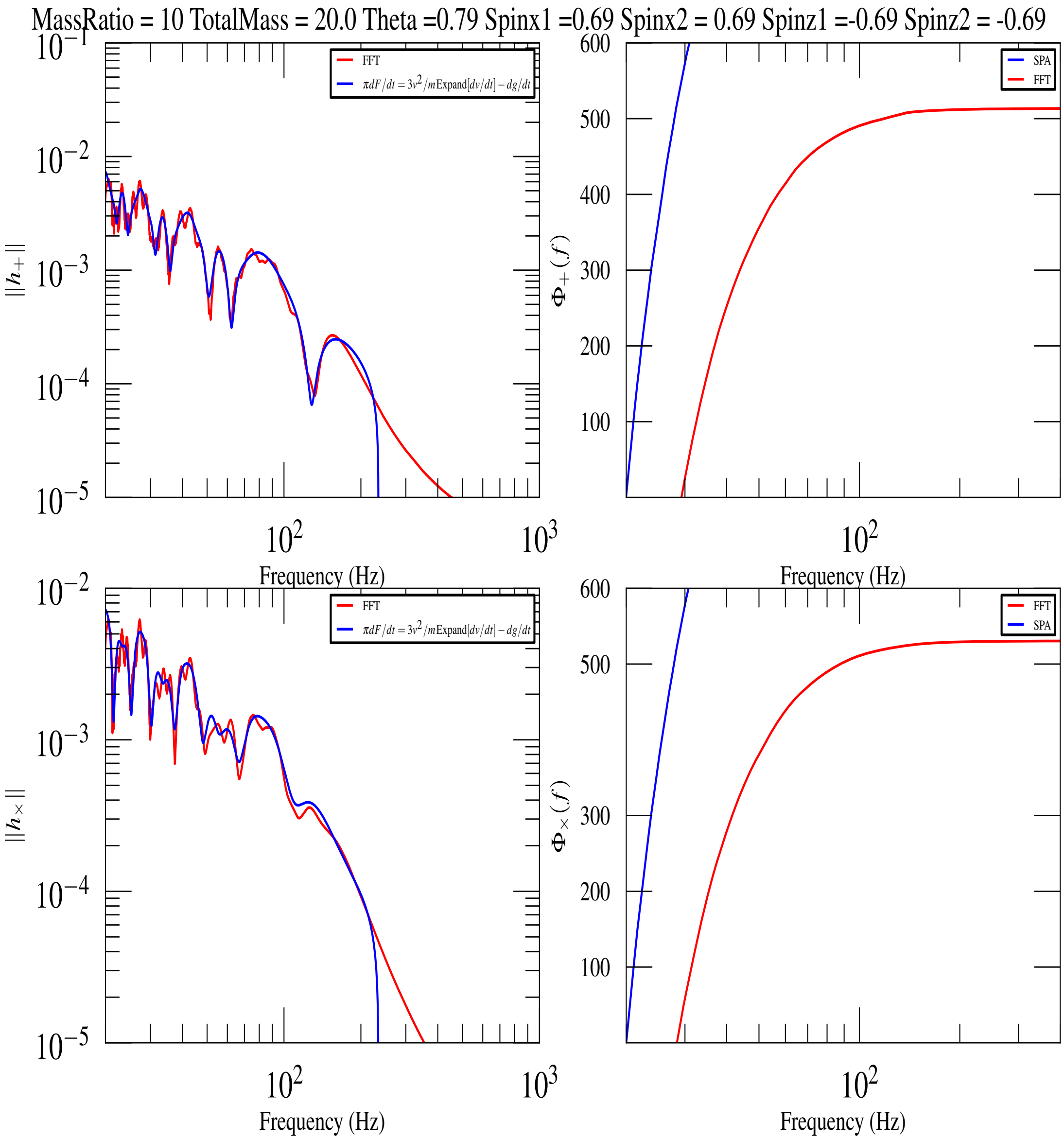

Figure 4.15: Above figure shows the Fourier domain gravitational waveform from binary balck hole system with the parameters mentioned on the top .In the above figure the left column shows the comparison of the amplitude of two polarization($h_+(v)$ and $h_\times(v)$) in Fourier domain, obtained using stationary phase approximation and numerical FFT. The right column shows a similar comparison for phase for the two polarization components.

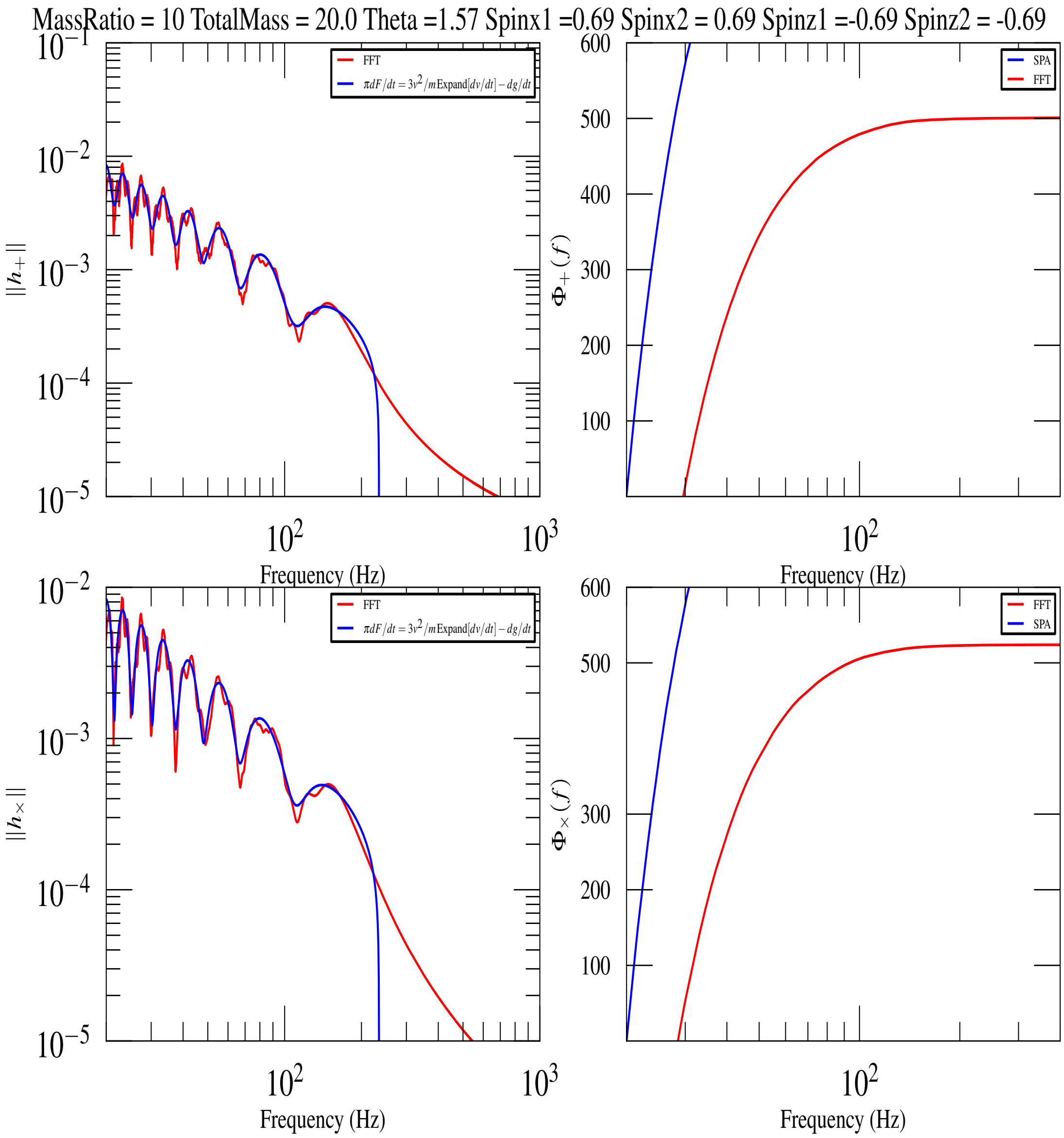

Figure 4.16: Above figure shows the Fourier domain gravitational waveform from binary balck hole system with the parameters mentioned on the top .In the above figure the left column shows the comparison of the amplitude of two polarization($h_+(v)$ and $h_\times(v)$) in Fourier domain, obtained using stationary phase approximation and numerical FFT. The right column shows a similar comparison for phase for the two polarization components.

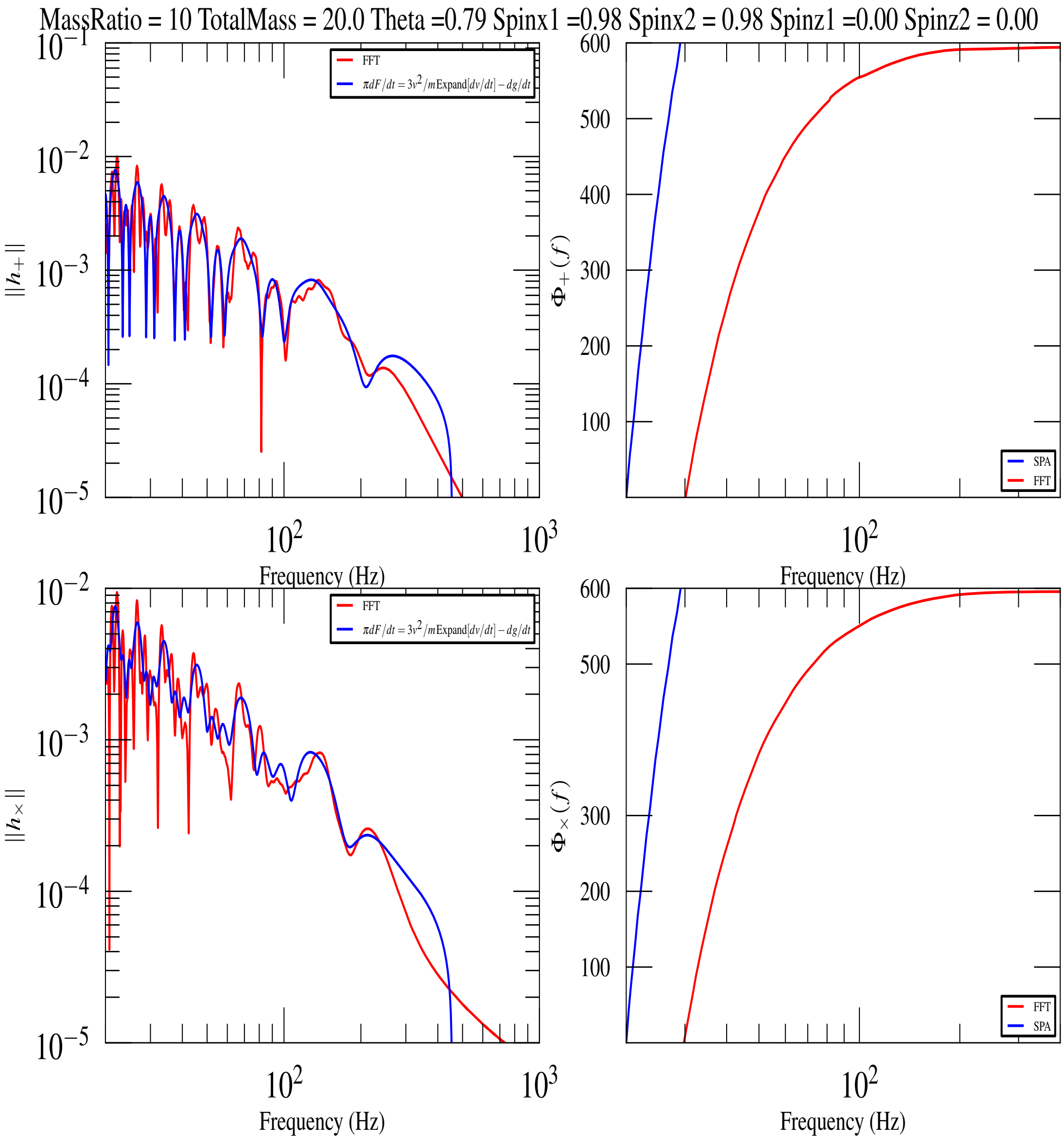

Figure 4.17: Above figure shows the Fourier domain gravitational waveform from binary balck hole system with the parameters mentioned on the top .In the above figure the left column shows the comparison of the amplitude of two polarization($h_+(v)$ and $h_\times(v)$) in Fourier domain, obtained using stationary phase approximation and numerical FFT. The right column shows a similar comparison for phase for the two polarization components.

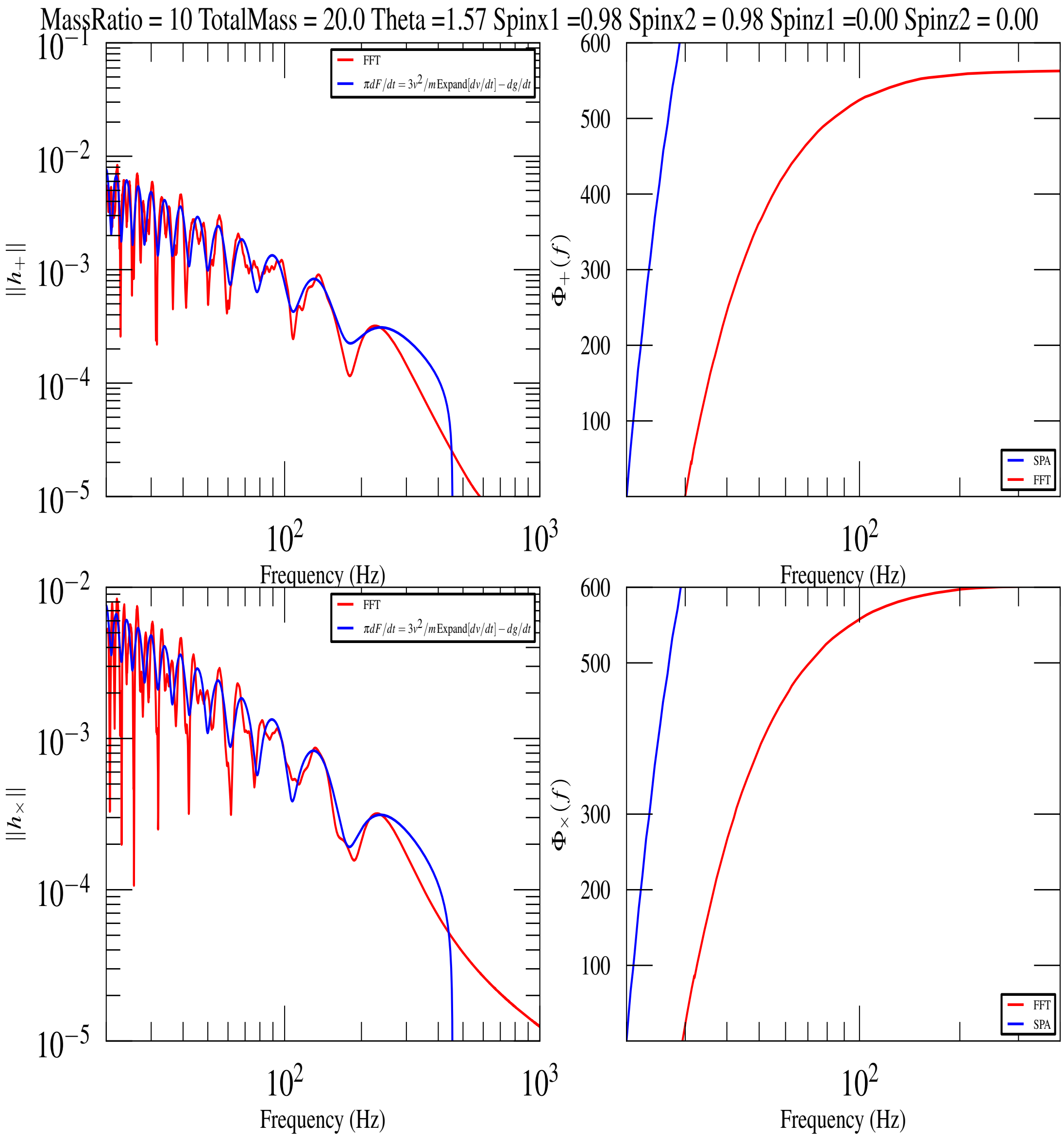

Figure 4.18: Above figure shows the Fourier domain gravitational waveform from binary balck hole system with the parameters mentioned on the top .In the above figure the left column shows the comparison of the amplitude of two polarization($h_+(v)$ and $h_\times(v)$) in Fourier domain, obtained using stationary phase approximation and numerical FFT. The right column shows a similar comparison for phase for the two polarization components.

Chapter 5

Summary

Astrophysical black holes are expected to have significant spins. If the spins are misaligned with the orbital angular momentum, the general-relativistic spin-orbit and spin-spin coupling will cause the spins to precess, which will introduce significant complexity in the observed gravitational-wave (GW) signal. In the adiabatic post-Newtonian approximation, the expected GW signals are typically computed by solving a set of 11 (or more) coupled ordinary differential equations that describe the time evolution of the spin and angular momentum vectors as well as the orbital frequency and phase. For the purpose of GW detection and parameter estimation, the Fourier transform of these waveforms are computed by means of Fast Fourier Transform algorithms. In this work, we present a semi-analytic frequency-domain post-Newtonian waveform family for generic spinning binaries. The evolution of spin and angular momentum vectors are computed by solving 6 ordinary differential equations in the frequency domain. Waveforms in the frequency domain are then computed using the stationary phase approximation(SPA). This provides a computationally efficient method for generating Fourier-domain templates for generic spinning binaries for GW detection and parameter estimation.

We see that our approximations of the SPA formula work well in case of binaries with lower mass ratios and which are not highly inclined. In case of binaries with high mass ratios, the effect of precession becomes important and the Fourier frequency needs to be computed more accurately. The terms in the equation (2.11) that appears due to precession are also highly oscillatory in nature, so we need to modify the formula of usual stationary phase approximation which take into account contribution from multiple stationary points. Work is in progress to improve the approximation and compute match with the FFT wave form as a target waveform. The match calculation is explained in section 2.2.

References

[1] Ajith, P. "Addressing the spin question in gravitational-wave searches: Waveform templates for inspiralling compact binaries with nonprecessing spins." Physical Review D 84.8 (2011): 084037.

[2] Damour, Thibault, Bala R. Iyer, and Bangalore S. Sathyaprakash. "Frequency-domain P-approximant filters for time-truncated inspiral gravitational wave signals from compact binaries." Physical Review D 62.8 (2000): 084036.

[3] Schutz, Bernard. A first course in general relativity. Cambridge university press, 2009.

[4] Blanchet, Luc. "Gravitational radiation from post-Newtonian sources and inspiralling compact binaries." Living Rev. Relativity 9 (2006).

[5]Sathyaprakash, B. S., and Bernard F. Schutz. "Physics, astrophysics and cosmology with gravitational waves." Living Rev. Relativity 12.2 (2009).

[6] Figure 2.1 courtesy : Chandra X-ray observatory(http://chandra.harvard.edu /resources/illustrations/neutronstars.html)

[6] Figure 1.1 courtesy : ([6] Figure 2.1 courtesy : Chandra X-ray observatory(http://chandra.harvard.edu
/resources/illustrations/neutronstars.html)

-